

## Neurotransmitter Switching Coupled to $\beta$ -Adrenergic Signaling in Sympathetic Neurons in Prehypertensive States

Emma N. Bardsley, Harvey Davis, Keith J. Buckler, David J. Paterson

**Abstract**—Single or combinatorial administration of  $\beta$ -blockers is a mainstay treatment strategy for conditions caused by sympathetic overactivity. Conventional wisdom suggests that the main beneficial effect of  $\beta$ -blockers includes resensitization and restoration of  $\beta_1$ -adrenergic signaling pathways in the myocardium, improvements in cardiomyocyte contractility, and reversal of ventricular sensitization. However, emerging evidence indicates that another beneficial effect of  $\beta$ -blockers in disease may reside in sympathetic neurons. We investigated whether  $\beta$ -adrenoceptors are present on postganglionic sympathetic neurons and facilitate neurotransmission in a feed-forward manner. Using a combination of immunocytochemistry, RNA sequencing, Förster resonance energy transfer, and intracellular  $\text{Ca}^{2+}$  imaging, we demonstrate the presence of  $\beta$ -adrenoceptors on presynaptic sympathetic neurons in both human and rat stellate ganglia. In diseased neurons from the prehypertensive rat, there was enhanced  $\beta$ -adrenoceptor-mediated signaling predominantly via  $\beta_2$ -adrenoceptor activation. Moreover, in human and rat neurons, we identified the presence of the epinephrine-synthesizing enzyme PNMT (phenylethanolamine-N-methyltransferase). Using high-pressure liquid chromatography with electrochemical detection, we measured greater epinephrine content and evoked release from the prehypertensive rat cardiac-stellate ganglia. We conclude that neurotransmitter switching resulting in enhanced epinephrine release, may provide presynaptic positive feedback on  $\beta$ -adrenoceptors to promote further release, that leads to greater postsynaptic excitability in disease, before increases in arterial blood pressure. Targeting neuronal  $\beta$ -adrenoceptor downstream signaling could provide therapeutic opportunity to minimize end-organ damage caused by sympathetic overactivity. (*Hypertension*. 2018;71:1226-1238. DOI: 10.1161/HYPERTENSIONAHA.118.10844.) • [Online Data Supplement](#)

**Key Words:** cardiovascular diseases ■ epinephrine ■ hypertension ■ sequence analysis, RNA ■ stellate ganglion

The myocardial  $\beta$ -adrenergic receptor ( $\beta$ AR) signaling pathway plays a pivotal role in the pathogenesis of many cardiovascular diseases. Chronic cardiac adrenergic activation and impaired myocardial cyclic nucleotide (cN) signaling, resulting from enhanced catecholaminergic neurotransmission, are well-established contributors to ventricular hypertrophy, arrhythmia, and cardiomyocyte apoptosis.<sup>1-3</sup> Sympathetic overactivity and vagal impairment (dysautonomia) are recurrent features in normotensive subjects with a familial predisposition for hypertension<sup>4,5</sup> and in animal models of this disease.<sup>6-8</sup> Moreover, patients with familial dysautonomia experience catecholaminergic supersensitivity, episodic hypertension, and have a high propensity for fatal cardiac events.<sup>9</sup>

$\beta$ -Blockers are a mainstay treatment for many cardiovascular diseases and stress-related events.<sup>10</sup> Chronic  $\beta$ -blocker therapy affords patients a wide-range of beneficial effects, including  $\beta_1$ AR resensitization and restoration of intracellular cN signaling pathways, improvements in cardiac myocyte contractility, and reversal of ventricular remodeling.<sup>1,3</sup> The precise mechanisms, however,

that mediate and sustain the beneficial effects of  $\beta$ -blockers in disease remain unclear,<sup>11,12</sup> although the presence of potentiating  $\text{G}\alpha_s$ -coupled presynaptic  $\beta$ ARs on presynaptic sympathetic terminals suggests a role for  $\beta$ -blockers in regulating cardiac-neuronal communication.<sup>13-22</sup> The Adrenaline Hypothesis of hypertension argues that small incremental increases in plasma adrenaline (epinephrine) enhance sympathetic activity through sustained activation of presynaptic sympathetic  $\beta$ ARs, leading to the development of hypertension.<sup>17,23,24</sup> Whether epinephrine synthesis occurs before the onset of hypertension is not known, as there is limited cellular and molecular data within the sympathetic stellate ganglia to confirm this idea.

In this study, we investigated whether sympathetic  $\beta$ ARs are present on human and rat sympathetic stellate ganglia (cervicothoracic ganglia, T1–T3) that preferentially innervate the heart.<sup>25-28</sup> We aimed to establish whether intracellular second messenger signaling coupled to presynaptic  $\beta$ ARs is impaired in prehypertensive states and contributes to altered  $\text{Ca}^{2+}$  and cN signaling before increases in arterial blood pressure. Finally,

Received January 6, 2018; first decision January 18, 2018; revision accepted March 26, 2018.

From the Wellcome Trust OXION Initiative in Ion Channels and Disease, Burdon Sanderson Cardiac Science Centre, Department of Physiology, Anatomy and Genetics, University of Oxford, United Kingdom.

The online-only Data Supplement is available with this article at <http://hyper.ahajournals.org/lookup/suppl/doi:10.1161/HYPERTENSIONAHA.118.10844/-DC1>.

Correspondence to Emma Nicole Bardsley or David James Paterson, Department of Physiology, Anatomy, and Genetics, University of Oxford, Oxford, OX1 3PT, United Kingdom. E-mail [emma.bardsley@dpag.ox.ac.uk](mailto:emma.bardsley@dpag.ox.ac.uk) or [david.paterson@dpag.ox.ac.uk](mailto:david.paterson@dpag.ox.ac.uk)

© 2018 The Authors. *Hypertension* is published on behalf of the American Heart Association, Inc., by Wolters Kluwer Health, Inc. This is an open access article under the terms of the [Creative Commons Attribution](#) License, which permits use, distribution, and reproduction in any medium, provided that the original work is properly cited.

*Hypertension* is available at <http://hyper.ahajournals.org>

DOI: 10.1161/HYPERTENSIONAHA.118.10844

we aimed to assess which neurotransmitters are present within the cardiac-sympathetic ganglia to test the idea that epinephrine may act as the preferential sympathetic neurotransmitter, predisposing to disease.

## Methods

### Data Accessibility

Our RNA sequencing (RNAseq) raw FastQ files are deposited in the National Center for Biotechnology Information short reads archive under Short Reads Archive number SRP132271, and our quasi-mapped data will be available under Gene Expression Omnibus accession number (GSE110197).

### Clinical Samples

For clinical samples, human stellate ganglia were kindly sent by Drs Ajijola, Ardell, and Shivkumar from University of California, Los Angeles, Cardiac Arrhythmia Center. Characteristics of human donors are included in the [online-only Data Supplement](#) (Table S1 in the [online-only Data Supplement](#)). The human study was approved by the University of California, Los Angeles, Institutional Review Board (approval no. 12-000701), and informed consent was obtained from all subjects.

### Animals

Young male prehypertensive spontaneously hypertensive rats (pre-SHRs) of 3.5 to 5.5 week old, 16- to 20-week-old adult male normotensive Wistar rats, and age-matched spontaneously hypertensive rats (SHRs) were obtained from Envigo, United Kingdom. The SHR strain displays normal blood pressure at 4 weeks of age, where increases in arterial blood pressure develop progressively from 5 to 6 weeks of age.<sup>29–36</sup> In this study, we used the Wistar rat strain as the normotensive control, given that Wistar rats are the progenitor strain from which the Wistar Kyoto was bred and the 2 strains display similar hemodynamic profiles at all ages.<sup>31,32,36–41</sup> In addition, neither strain display a sympathetic  $\text{Ca}^{2+}$  phenotype (Figure S1A), making the Wistar a suitable control in this study. All rats were housed in standard plastic cages, and artificial lighting was fixed to a natural 12-hour light/dark cycle. Food and water were available ad libitum. All experiments were performed in accordance with the UK Home Office Animal Scientific Procedures Act 1986 and approved by the University of Oxford (PPL 30/3131; David J. Paterson). An expanded Materials and Methods section is available in the [online-only Data Supplement](#) for neuronal culture methodology, immunocytochemistry, RNAseq, Förster resonance energy transfer (FRET),  $\text{Ca}^{2+}$  imaging, and high-pressure liquid chromatography coupled to electrochemical detection protocols.

## Results

### Rat and Human Sympathetic Stellate Ganglia Express $\beta_1$ and $\beta_2$ Adrenoceptors

We sequenced the transcriptome of the sympathetic stellate ganglia from 16-week-old male Wistar rats ( $n=4$ ) and SHR ( $n=4$ ). At 16 weeks, it is well-established that SHR display hypertension and sympathetic hyperactivity.<sup>6,29–31,33,35,36,42</sup> Using quasi-mapping RNAseq<sup>43</sup> and quantitative real-time (qRT)-polymerase chain reaction (PCR), we identified the presence of  $\beta_1$ AR (*Adrb1*) and  $\beta_2$ AR (*Adrb2*) mRNA transcripts, in addition to  $\alpha_{2A}$ AR (*Adra2a*) and tyrosine hydroxylase (*Th*) mRNA transcripts, markers of presynaptic sympathetic neurons, respectively (Figure 1A; Figure S1). We selected the  $\alpha_{2A}$ AR isoform as an indicator of presynaptic neuronal phenotype based on reports that the  $\alpha_{2A}$ AR primarily regulates presynaptic sympathetic activity.<sup>44</sup> The  $\alpha_{2C}$ AR isoform plays a secondary role in regulating presynaptic norepinephrine release,<sup>44</sup> whereas the

$\alpha_{2B}$ AR isoform has a preferential role within the vasculature.<sup>44</sup> The mRNA expression for  $\alpha_{2A}$ AR was also found to be significantly higher than  $\alpha_{2C}$ AR expression identified by RNAseq (data not shown). Using RNAseq, we found that *Adrb2* mRNA expression was significantly lower in SHR ganglia compared with Wistar (Figure 1A; Figure S1C;  $P_{\text{adj}}=0.00945$ ). Data points represent mean raw counts $\pm$ SEM (Figure 1A).

The presence of *Adrb1*, *Adrb2*, *Adra2a*, and *Th* mRNA transcripts was identified and quantified by quantitative real time PCR (qRT-PCR) using RNA extracted from 4-week pre-SHR and Wistar rats ( $n=3$  rats/group, unpooled; Figure S1D) and 16-week SHR and Wistar rats ( $n=4$  rats/group, unpooled; Figure S1D). qRT-PCR data were analyzed using the  $\Delta\Delta C_T$  method, where raw counts in both strains were first normalized to a control housekeeping gene *B2m*, and the difference in counts between SHR and Wistar was calculated.<sup>45</sup> Data points represent  $\log_2$  (fold change) $\pm$ SEM. There was no significant difference in the levels of mRNA for *Adrb1*, *Adrb2*, *Adra2a*, or *Th* between strains or between age groups by qRT-PCR although the trend for a reduction in *Adrb2* expression remained.

Sandwich ELISAs were used to quantify the relative protein expression of  $\beta_1$ AR and  $\beta_2$ ARs in postganglionic sympathetic neurons obtained from 3- to 5-week-old normotensive pre-SHR and Wistar rats (Figure 1B; 32 stellates, 16 rats/group, pooled) or 19- to 20-week-old SHR and age-matched Wistar rats (Figure 1C; 20 stellates, 10 rats/group, pooled). The ELISA assays were biologically powered where 20 to 32 stellates were used per sample; however, the stellates tissue was pooled to obtain an adequate protein concentration for the ELISA assays, therefore no statistical comparisons were made. Data points indicate mean $\pm$ SEM (of 3–4 technical replicates).

In 4 stellate ganglia samples obtained from 3 human donors (2 left stellates, 2 right stellates, unpooled), qRT-PCR confirmed the presence of mRNA transcripts encoding  $\beta_1$ AR (*Adrb1*) and  $\beta_2$ AR (*Adrb2*; S1E). Ganglia were  $\alpha_{2A}$ AR (*Adra2a*) positive, confirming a presynaptic phenotype. Samples were normalized to a control housekeeping gene *B2m* (3 replicates) using the  $\Delta C_T$  method.<sup>45</sup> Data points represent normalized counts $\pm$ SEM. ELISAs confirmed the expression of  $\beta_1$ AR (516 $\pm$ 99.17 pg/mL) and  $\beta_2$ AR (340 $\pm$ 104.3 pg/mL) in 3 human stellates obtained from 2 patients (Figure 1D; pooled, 6 replicates). Immunocytochemistry confirmed the expression of  $\beta_1$ AR and  $\beta_2$ AR on TH-positive neurons from 3- to 5-week-old control rats (Figure 1E and 1F; respectively) and SHR (data not shown).

### $\beta$ AR-Evoked cAMP Generation, PKA Activity, and $[\text{Ca}^{2+}]_i$ Are Enhanced in Pre-SHR Neurons

To determine whether the presence of presynaptic  $\beta$ ARs on sympathetic ganglia plays a functional role in modulating intracellular cN signaling pathways, we used FRET to quantify the relative levels of cAMP and PKA (protein kinase A) activity in response to a relatively nonselective  $\beta$ AR agonist, isoprenaline. To assess whether  $\beta$ AR-mediated cAMP generation facilitated signaling via the canonical cAMP–PKA– $\text{Ca}^{2+}$  pathway, we used the loss-of-FRET sensor Epacs1-H187 (EpacH187)<sup>46</sup> to measure changes in intracellular cAMP. Isoprenaline administration at 10 nmol/L led to significantly greater cAMP generation in pre-SHR (55.6% $\pm$ 16.8%)

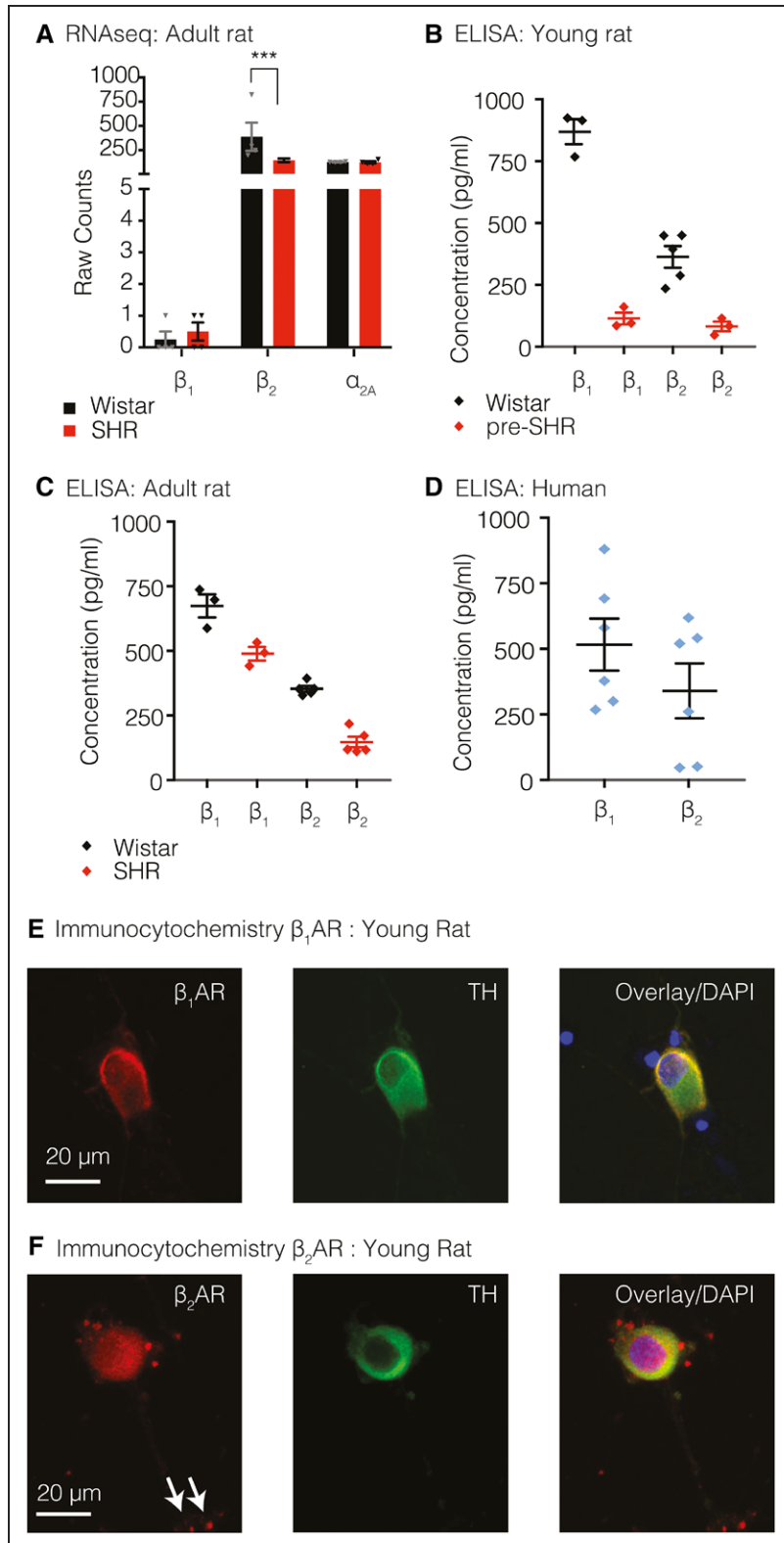


**Figure 1.** Rat sympathetic stellate ganglia express  $\beta_1$ - and  $\beta_2$ -adrenergic receptors (ARs). Using RNA sequencing, we identified the presence of  $\beta_1$ AR (*Adrb1*),  $\beta_2$ AR (*Adrb2*), and  $\alpha_{2A}$ AR (*Adra2a*) mRNA transcripts (**A**) from 16-wk-old male Wistar rats ( $n=4$ ) and SHR ( $n=4$ ). *Adrb2* expression was significantly lower in SHR ganglia compared with Wistar ( $P$ ,  $\text{adj}=0.00945$ ; Salmon-DESeq2 method). There was no significant difference in the levels of mRNA for *Adrb1* or *Adra2a* between strains or between age groups. Data points represent raw counts $\pm$ SEM for each transcript (**A**). ELISAs confirmed protein expression of  $\beta_1$ AR and  $\beta_2$ ARs in 3.5- to 5-wk-old rat neurons (32 stellates, 16 animals/group) and 20-wk-old neurons (20 stellates, 10 animals/group); however, no statistical tests were conducted as stellates were pooled into a single sample to obtain adequate protein concentrations for the ELISA assays. In young rat stellates (**B**), the concentration of  $\beta_1$ AR protein was calculated as  $869.1\pm50.6$  pg/mL (Wistar) and  $114.2\pm23.7$  pg/mL (pre-SHR).  $\beta_2$ AR protein expression was calculated as  $363.5\pm43.6$  pg/mL (Wistar) and  $82.2\pm20.0$  pg/mL (pre-SHR). In adult rat stellates (**C**),  $\beta_1$ AR expression was calculated as  $674.1\pm44.6$  pg/mL (Wistar) and  $489.4\pm26.3$  pg/mL (SHR).  $\beta_2$ AR protein expression quantified as  $353.3\pm11.2$  pg/mL (Wistar) and  $147.4\pm20.7$  pg/mL (SHR). Data points depict mean $\pm$ SEM of 3 to 4 technical replicates.  $\beta_1$ AR ( $516\pm99.17$  pg/mL) and  $\beta_2$ AR ( $340\pm104.3$  pg/mL) expression was also detected in stellate ganglia from human donors. Data points represent mean $\pm$ SEM (6 replicates), from 3 pooled stellates obtained from 2 patients (**D**). Immunocytochemistry depicts  $\beta_1$ AR (**E**) and  $\beta_2$ AR (**F**) expression on TH (tyrosine hydroxylase)-positive neurons from 4-wk control rats. White arrows demonstrate the localization of  $\beta_2$ AR on synaptic terminals.

compared with that measured in Wistar neurons ( $7.1\%\pm1.4\%$ ; 2-way ANOVA;  $P<0.0001$ ) that was also observed at higher concentrations of isoprenaline (Figure 2A and 2B). PKA activity was measured using the gain-of-FRET sensor AKAR4.<sup>47</sup> Using the same concentration of isoprenaline (10 nmol/L), we found that PKA activity was significantly higher in

pre-SHR ( $26.1\%\pm5.4\%$ ) versus Wistar neurons ( $4.5\%\pm1.1\%$ ; 2-way ANOVA;  $P<0.0001$ ), which was also observed at 100 nmol/L isoprenaline (Figure 2C and 2D). Raw YFP (yellow fluorescent protein) and CFP (cyan fluorescent protein) fluorescence traces as emitted from the cytosolic loss-of FRET sensor EpacH187 and the gain-of-FRET sensor AKAR4 in



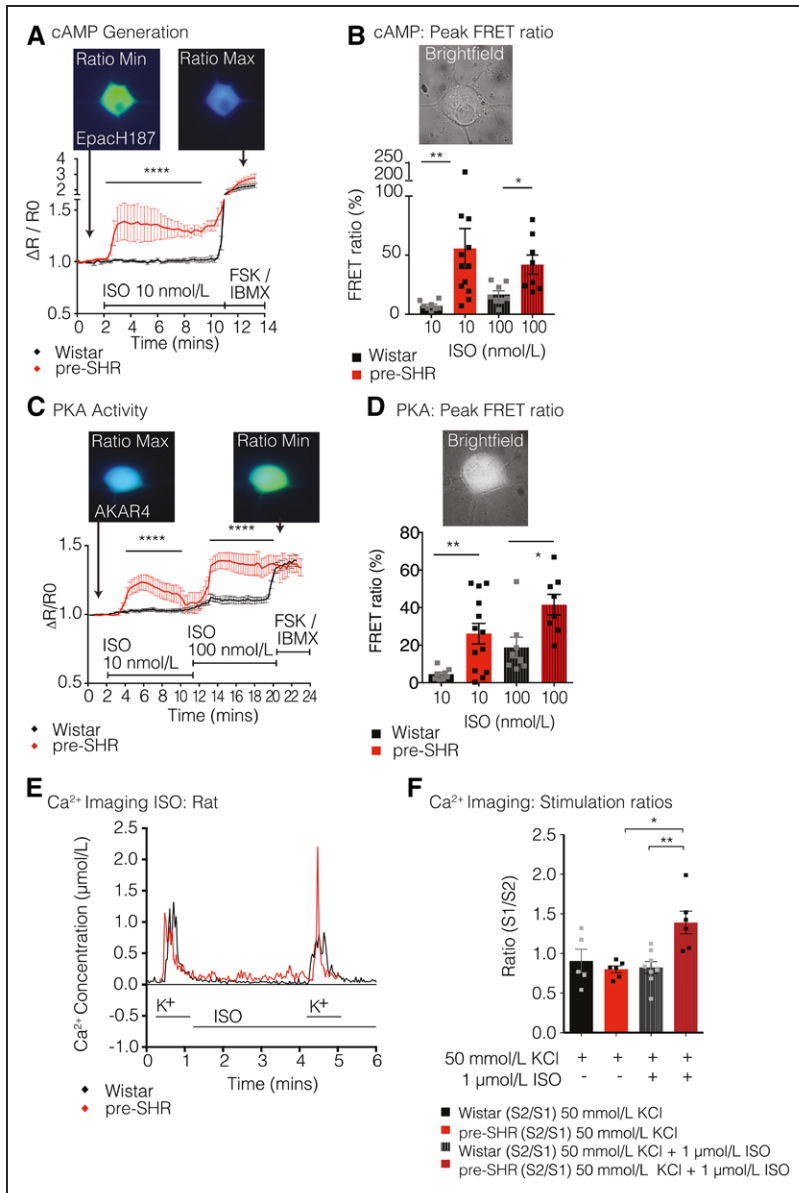


**Figure 2.**  $\beta$ -Adrenergic receptor ( $\beta$ AR) stimulation increases cAMP–PKA– $\text{Ca}^{2+}$  signaling in pre-SHR neurons. Isoprenaline (ISO) generated significantly higher levels of cAMP at 10 nmol/L (**A**) in pre-SHR ( $55.6\% \pm 16.8\%$ ;  $n=12$ ) compared with Wistar neurons ( $7.1\% \pm 1.4\%$ ;  $n=8$ ; 2-way ANOVA;  $P<0.0001$ ) and at 100 nmol/L (**B**) in pre-SHR ( $42.0\% \pm 8.2\%$ ;  $n=8$ ) vs Wistar ( $16.8\% \pm 3.2\%$ ;  $n=8$ ; 2-way ANOVA;  $P<0.0001$ ). ISO increased PKA activity to a significantly greater extent at 10 nmol/L (**C**) in pre-SHR ( $26.1\% \pm 5.5\%$ ;  $n=13$ ) vs Wistar neurons ( $4.5\% \pm 1.1\%$ ;  $n=8$ ; 2-way ANOVA;  $P<0.0001$ ) and at 100 nmol/L (**D**) in pre-SHR ( $41.5\% \pm 5.5\%$ ;  $n=8$ ) vs Wistar ( $18.8\% \pm 5.4\%$ ;  $n=8$ ; 2-way ANOVA;  $P<0.0001$ ). Cells that did not respond appropriately to forskolin (FSK, 25  $\mu\text{mol/L}$ ) and IBMX (3-isobutyl-1-methylxanthine; 100  $\mu\text{mol/L}$ ) were excluded from the final analysis.  $\text{Ca}^{2+}$  imaging was conducted on neurons obtained from 4-wk rats using Indo-1AM (**E** and **F**). Wistar and pre-SHR neurons ( $n=8$ , 6, respectively) were exposed to 2 KCl challenges (50 mmol/L; stimulations 1 and 2) where stimulation 2 was conducted in the presence of ISO (1  $\mu\text{mol/L}$ ). Time-controlled experiments were performed in the absence of ISO (Wistar,  $n=5$ ; and pre-SHR  $n=6$ ). There was significantly higher  $[\text{Ca}^{2+}]_i$  evoked in the presence of ISO in pre-SHR neurons compared with Wistar neurons (unpaired Student  $t$  test;  $P=0.0027$ ). Bar charts represent mean  $\pm$  SEM. FRET indicates Förster resonance energy transfer.

response to isoprenaline (10–100 nmol/L) are presented in the [online-only Data Supplement](#) (Figure S2A and S2B).

To assess whether isoprenaline-dependent  $\beta$ AR activation enhances intracellular  $\text{Ca}^{2+}$  ( $[\text{Ca}^{2+}]_i$ ), we measured responses to KCl in the absence or presence of isoprenaline.  $\text{Ca}^{2+}$  recordings were obtained using Indo-1AM labeled sympathetic neurons from 4-week pre-SHR and Wistar rats. In pre-SHR stellate neurons, KCl stimulation in the presence of isoprenaline led to significantly higher  $[\text{Ca}^{2+}]_i$  than KCl stimulations alone (Figure 2E and 2F;  $P=0.0272$ ). There was significantly higher KCl-evoked  $[\text{Ca}^{2+}]_i$  in the presence of isoprenaline in pre-SHR neurons compared with that recorded in control neurons (Figure 2E and 2F;  $P=0.0027$ ). A time-controlled example trace is shown in the [online-only Data Supplement](#) (Figure S2C).

### Relative Contribution of $\beta_1$ AR and $\beta_2$ AR Signaling in Neuronal cAMP Generation

To ascertain whether the observed increases in isoprenaline-evoked cAMP occurs predominantly through either  $\beta_1$ AR or

$\beta_2$ AR activation, cells were challenged with either a  $\beta_1$ AR agonist (dobutamine, 50  $\mu\text{mol/L}$ ) after  $\beta_2$ AR blockade with ICI-118,551 (ICI, 10 nmol/L) or in alternative experiments, administration of a  $\beta_2$ AR agonist (salbutamol, 10  $\mu\text{mol/L}$ ) after  $\beta_1$ AR antagonism (metoprolol, 100 nmol/L). Administration of the  $\beta_1$ AR agonist dobutamine led to significantly greater cAMP generation in pre-SHR ( $15.82\% \pm 2.8\%$ ) compared with Wistar neurons ( $-0.31\% \pm 2.4\%$ ; 2-way ANOVA;  $P<0.0001$ ; Figure 3A and 3C).

We observed that in Wistar neurons, administration of dobutamine did not increase cAMP from baseline. Administration of the  $\beta_2$ AR agonist salbutamol also led to a significantly greater cAMP generation in pre-SHR ( $63.8\% \pm 16.6\%$ ) compared with Wistar neurons ( $38.6\% \pm 5.2\%$ ; 2-way ANOVA;  $P<0.0001$ ; Figure 3B and 3C). There was significantly higher peak salbutamol-evoked cAMP compared with dobutamine-evoked cAMP in Wistar ( $P<0.0001$ ; Mann–Whitney) and in pre-SHR neurons ( $P=0.0173$ , unpaired 2-tailed Student  $t$  test), highlighting a greater contribution of  $\beta_2$ AR versus  $\beta_1$ AR in generating cAMP, regardless of strain (C).

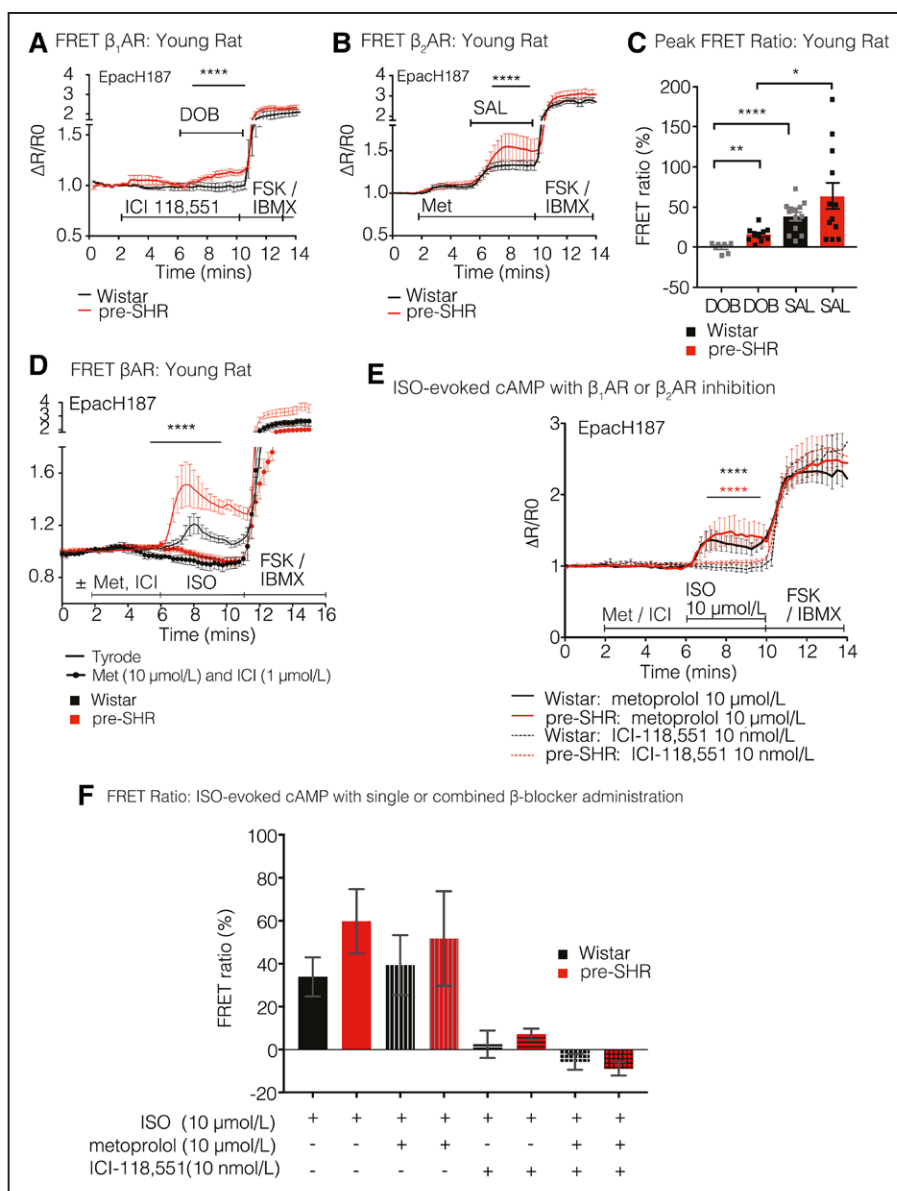


**Figure 3.** Relative contribution of presynaptic  $\beta_1$ -adrenergic receptor (AR) and  $\beta_2$ AR in neuron cAMP generation. For measurements of cAMP generation, 4-wk control and age-matched pre-SHR neurons were transduced with the EpacH187 FRET biosensor. Cells were stimulated with a  $\beta_1$ AR agonist, dobutamine (DOB, 50  $\mu$ mol/L) after  $\beta_2$ AR inhibition with a selective antagonist, ICI-118,551 (ICI, 10 nmol/L) that led to a significantly greater increase in cAMP generation in pre-SHR ( $15.82 \pm 2.8\%$ ;  $n=5$ ) compared with Wistar neurons ( $-0.31 \pm 2.4\%$ ;  $n=10$ ; 2-way ANOVA;  $P<0.0001$ ). In Wistar neurons, administration of DOB did not increase cAMP from baseline (A). In alternative experiments, neurons were stimulated with a  $\beta_2$ AR agonist salbutamol (SAL, 10  $\mu$ mol/L) after  $\beta_1$ AR inhibition with a selective antagonist, metoprolol (MET, 100 nmol/L). SAL administration led to a greater increase in cAMP generation in pre-SHR ( $63.8 \pm 16.6\%$ ;  $n=12$ ) compared with Wistar neurons ( $38.6 \pm 5.2\%$ ;  $n=13$ ; 2-way ANOVA;  $P<0.0001$ ; B). Peak FRET ratios (%) evoked by DOB or SAL were calculated (C). SAL generated significantly higher cAMP levels, than that evoked by DOB in Wistar ( $P<0.0001$ , Mann-Whitney) and in pre-SHR PGSNs ( $P=0.0173$ , unpaired 2-tailed Student  $t$  test). To confirm that ISO-evoked cAMP was acting downstream of  $\beta$ AR activation, we tested ISO-evoked cAMP in the absence and presence of a combination of  $\beta_1$ AR and  $\beta_2$ AR antagonists (ISO, 10  $\mu$ mol/L; MET, 10  $\mu$ mol/L; ICI, 1  $\mu$ mol/L, respectively) or selective blockade of either  $\beta_1$ AR (MET, 10  $\mu$ mol/L) or  $\beta_2$ AR (ICI, 10 nmol/L). The dual combination of  $\beta$ -blockers abolished cAMP generation in both pre-SHR ( $n=6$ ) and Wistar neurons ( $n=6$ ), demonstrating that ISO-dependent cAMP generation is dependent on  $\beta$ AR activation (D). There was significantly greater inhibition of cAMP after  $\beta_2$ AR compared with  $\beta_1$ AR inhibition in Wistar ( $P<0.0001$ ; 2-way repeated measures ANOVA) and pre-SHR neurons ( $P<0.0001$ ; 2-way repeated measures ANOVA), suggesting that  $\beta_2$ AR plays a predominant role in cAMP generation, regardless of strain (E). Peak FRET responses are depicted (F).

To confirm that isoprenaline-evoked cAMP is acting through  $\beta_1$ AR and  $\beta_2$ ARs rather than inducing off-target effects, we tested isoprenaline-evoked cAMP in the absence and presence of a combination of  $\beta_1$ AR and  $\beta_2$ AR antagonists (isoprenaline, 10  $\mu$ mol/L; metoprolol, 10  $\mu$ mol/L; ICI,

1  $\mu$ mol/L, respectively). The combination of  $\beta_1$ AR and  $\beta_2$ AR antagonists abolished cAMP generation entirely in response to a high concentration of isoprenaline in both pre-SHR ( $n=6$ ) and Wistar neurons ( $n=6$ ), demonstrating that isoprenaline-dependent cAMP generation is dependent on selective

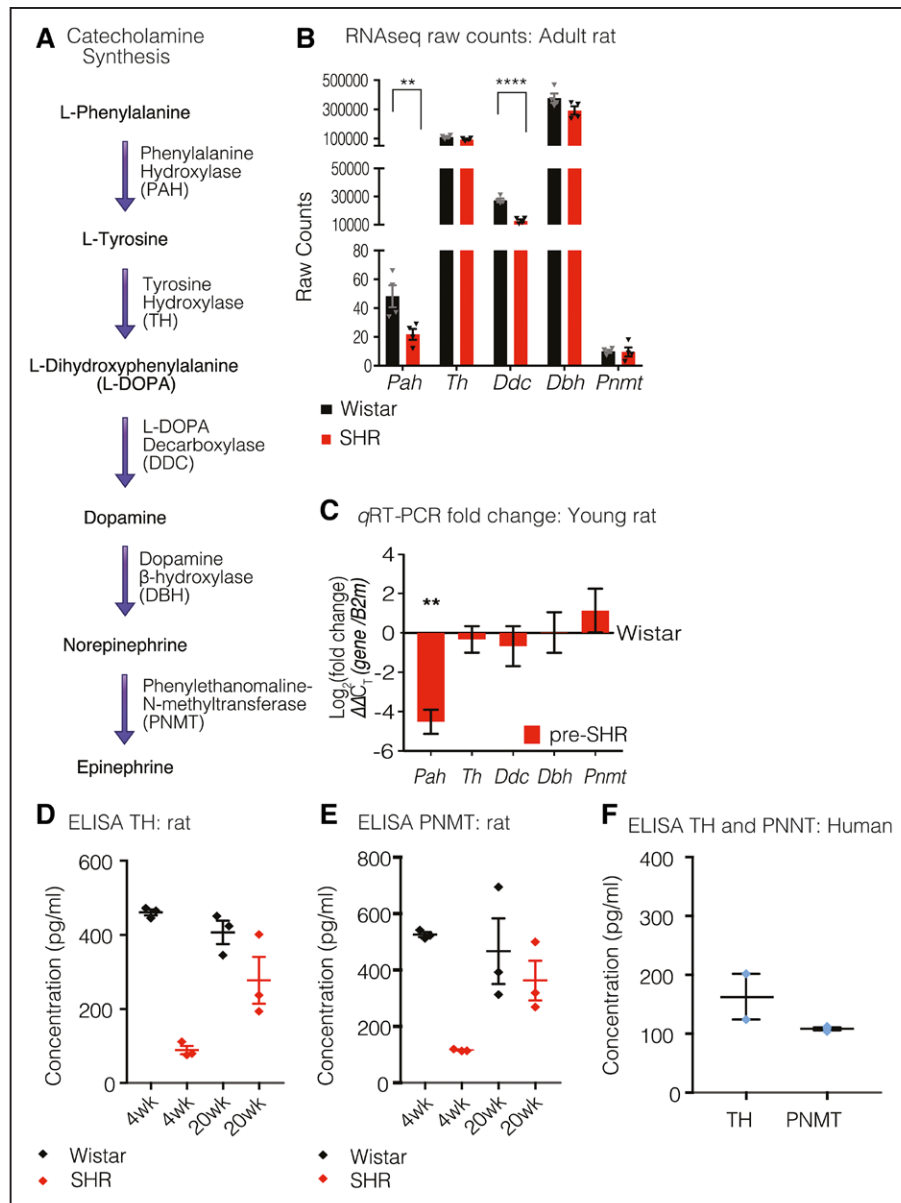


**Figure 4.** The epinephrine-synthesizing enzyme PNMT (phenylethanolamine-N-methyltransferase) is present in rat and human stellate ganglia. The catecholamine synthesis pathway is outlined (A). RNA sequencing (RNAseq) revealed mRNA transcripts that encode the enzymes required for norepinephrine (NE) synthesis: phenylalanine hydroxylase (*Pah*), tyrosine hydroxylase (*Th*), L-DOPA decarboxylase (*Ddc*), dopamine β-hydroxylase (*Dbh*; B). We also identified the transcript that encodes *Pnmt* required for the conversion of NE to epinephrine (Epi). *Pah* and *Ddc* mRNA expressions as determined by RNAseq were significantly lower in SHR neurons ( $P_{adj}=0.0719$ , *Pah*;  $6.64 \times 10^{-15}$ , *Ddc*; Salmon-DESeq2). Data depicts raw counts  $\pm$  SEM (B). Transcript expression was validated via quantitative real-time polymerase chain reaction (qRT-PCR) using RNA extracted from 4-wk Wistar ( $n=4$ ) and pre-SHR ( $n=4$ ) ganglia (C). For qRT-PCR analyses, genes were normalized to the housekeeping gene (*B2m*), and SHR counts were normalized to Wistar using the  $\Delta\Delta C_t$  method. There was a significant (4-fold) decrease in *Pah* in pre-SHR neurons (C;  $P=0.0098$ , unpaired 2-tailed Student *t* test). SHR (red bars) are depicted relative to number of counts calculated from Wistar samples (*x* axis). The protein concentration for TH (D) was quantified in 4-wk Wistar ( $460.9 \pm 7.979$  pg/mL), pre-SHR ganglia ( $89.12 \pm 11.37$  pg/mL), 20-wk Wistar ( $406.6 \pm 31.57$  pg/mL), and SHR ganglia ( $277.5 \pm 63.03$  pg/mL). PNMT protein expression was also quantified (E) in 4-wk Wistar ( $525.7 \pm 8.69$  pg/mL), pre-SHR ganglia ( $117 \pm 3.73$  pg/mL), 20-wk Wistar ( $466.7 \pm 116.2$  pg/mL), and SHR ganglia ( $362.7 \pm 70.08$  pg/mL). Data represent mean  $\pm$  SEM (2–3 technical replicates). We confirmed the protein expression of TH ( $163 \pm 38.83$  pg/mL) and PNMT ( $108.4 \pm 2.386$  pg/mL) in human stellates (F). Data points represent mean  $\pm$  SEM (2–3 replicates) from 3 pooled stellates obtained from 2 patients. Where stellates were pooled to obtain adequate protein concentrations, no statistical tests were conducted.

$\beta_1$ AR and  $\beta_2$ AR activation (Figure 3D). To support these observations, we also selectively inhibited  $\beta_1$ AR (metoprolol, 10  $\mu$ mol/L) or  $\beta_2$ AR (ICI, 10 nmol/L) and measured the resulting cAMP generation in response to isoprenaline (10  $\mu$ mol/L).  $\beta_2$ AR blockade reduced isoprenaline-evoked cAMP generation to a greater extent than  $\beta_1$ AR blockade

in both Wistar and pre-SHR neurons, confirming our previous observations for a preferential effect of  $\beta_2$ AR versus  $\beta_1$ AR mediated signaling in postganglionic sympathetic neurons (Figure 3E and 3F). We measured a slight but significantly greater cAMP generation in pre-SHR versus Wistar neurons in the presence of either metoprolol ( $P=0.0472$ )

or ICI ( $P<0.001$ ) using 2-way repeated measure ANOVAs; however, the peak FRET responses themselves were not different significantly between strains (Figure 3F). The selectivity and specificity of the selected  $\beta_1$ AR and  $\beta_2$ AR agonists (dobutamine and salbutamol, respectively) and the  $\beta_1$ AR and  $\beta_2$ AR antagonists (metoprolol and ICI) have been previously reported.<sup>48–51</sup>

### Epinephrine-Synthesizing Enzyme PNMT Is Present in Rat and Human Stellate Ganglia

RNAseq was performed to obtain an overview of the transcriptome in stellate ganglia obtained from 16-week-old male SHR ( $n=4$ ) and Wistar rats ( $n=4$ ). We identified the presence of mRNA transcripts-encoding enzymes required for norepinephrine synthesis (Figure 4A): phenylalanine hydroxylase (*Pah*), *Th*, L-DOPA decarboxylase (*Ddc*), dopamine  $\beta$ -hydroxylase (*Dbh*). Furthermore, RNAseq identified the presence of the mRNA transcript encoding phenylethanolamine-N-methyltransferase (*Pnmt*), the enzyme required for the conversion of norepinephrine to epinephrine in both Wistar and SHR stellate ganglia. In the RNAseq data set, *Pah* and *Ddc* mRNA transcript expression were also shown to be significantly lower in SHR neurons (Figure 4B; Figure S3A;  $P_{\text{adj}}=0.0719$ ;  $6.64\times 10^{-15}$ , *Pah*, *Ddc*, respectively). These findings were validated in 4-week Wistar and pre-SHR by qRT-PCR, and a significant  $\approx 4$ -fold reduction in *Pah* expression was observed in pre-SHR ganglia (Figure 4C;  $P=0.0098$ ). Data were normalized to a control housekeeping gene (*B2m*), and SHR gene counts were subsequently normalized to Wistar using the  $\Delta\Delta C_T$  method. Data are presented as  $\text{Log}_2$  (fold change).<sup>45</sup> Using the same method, we also confirmed the presence of *Pnmt* and *Th* by qRT-PCR in neurons from 16-week Wistar and SHR (Figure S3B). There was no significant difference in mRNA expression of either *Th* or *Pnmt* between age groups or between phenotypes. ELISA assays confirmed protein expression of TH (Figure 4D) and PNMT (Figure 4E) in stellate ganglia from 4-week pre-SHR, 20-week-old SHR, and age-matched Wistar rats. The ELISA assays were high-powered

biologically, where 20 to 32 stellates were used per sample; however, stellates were pooled to obtain adequate protein concentrations for the ELISA assays, therefore no statistical comparisons were made. Data points indicate mean $\pm$ SEM (of 2–3 technical replicates).

To assess whether the presence of PNMT in sympathetic stellate ganglia is conserved in higher species, we obtained stellate ganglia from male human donors. qRT-PCR demonstrated the presence of both *Th* and *Pnmt* mRNA transcripts in human sympathetic stellate ganglia (Figure S3C). Data were normalized to a control housekeeping gene *B2m* using the  $\Delta C_T$  method<sup>45</sup> and expressed as normalized count values (3 patients, 4 stellates). We also used ELISAs to confirm protein expression of both TH and PNMT in human stellate samples (Figure 4F). Data points represent mean $\pm$ SEM (2–3 replicates) from 3 pooled stellates obtained from 2 patients.

### Epinephrine Is Released From Pre-SHR but Not Wistar Whole-Stellate Ganglia

After the identification of PNMT, we investigated whether epinephrine is released from the whole rat stellate ganglia under basal conditions or with electric field stimulation. We measured significantly greater total norepinephrine content in homogenized Wistar stellates ( $43.3\pm 2.173$  pg;  $n=8$ ) compared with pre-SHR stellate ganglia ( $29.82\pm 6.366$  pg;  $n=4$ ;  $P=0.0294$ ). In the same homogenate, we measured a greater content of epinephrine in pre-SHR ganglia ( $14.14\pm 5.399$  pg) compared with that measured in Wistar stellates ( $3.937\pm 0.820$  pg;  $P=0.0019$ ), suggesting that a significant amount of norepinephrine is converted to epinephrine in prehypertensive states (Figure 5A).

We also investigated whether epinephrine is released from rat stellate ganglia with electric stimulation (Figure 5B). Electrically evoked concentrations of norepinephrine were significantly higher in samples obtained from pre-SHR ( $4.32\pm 1.523$  pg;  $n=4$ ) versus Wistar ganglia ( $1.477\pm 0.316$  pg;  $n=8$ ;  $P=0.0396$ ). Moreover, in the same samples, the concentrations of electrically evoked epinephrine were significantly

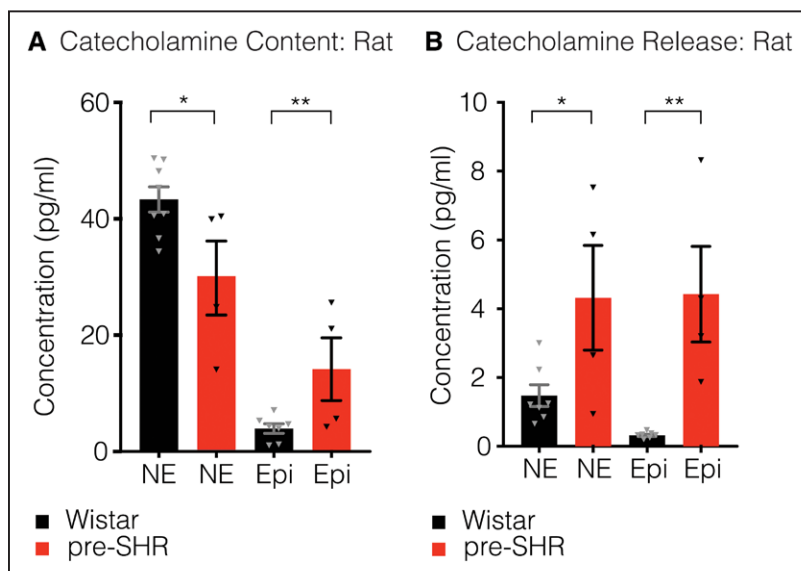


**Figure 5.** Epinephrine (Epi) is released from pre-SHR but not Wistar whole-stellate ganglia. Using high-pressure liquid chromatography coupled to electrochemical detection, we measured significantly higher total norepinephrine (NE; **A**) in Wistar ( $43.3\pm 2.173$  pg;  $n=8$ ) compared with pre-SHR neurons ( $29.82\pm 6.366$  pg;  $n=4$ ; unpaired 2-tailed Student *t* test;  $P=0.0294$ ). In the same stellate samples (**A**), we also measured a significantly greater total content of Epi in pre-SHR ( $14.14\pm 5.399$  pg) compared with that measured in Wistar ganglia ( $3.937\pm 0.820$  pg; unpaired 2-tailed Student *t* test;  $P=0.0019$ ). Electric field stimulation of whole-rat stellate ganglia led to the release of NE (**B**) that was significantly higher in samples obtained from pre-SHR ( $4.32\pm 1.523$  pg) vs Wistar ganglia ( $1.477\pm 0.316$  pg; unpaired 2-tailed Student *t* test;  $P=0.0396$ ). The concentrations of neurally-mediated Epi release (**B**) were also significantly higher in pre-SHR ( $4.424\pm 1.391$  pg;  $n=4$ ) compared with Wistar stellates ( $0.3201\pm 0.0325$  pg;  $n=8$ ; unpaired 2-tailed Student *t* test;  $P=0.0028$ ).



higher in pre-SHR ganglia ( $4.424 \pm 1.391$  pg) compared with that measured in Wistar stellates ( $0.3201 \pm 0.0325$  pg;  $P=0.0396$ ).

## Discussion

In this study, we have obtained evidence for  $\beta_1$ AR and  $\beta_2$ AR mRNA and protein expression on presynaptic postganglionic sympathetic neurons from human and rat ganglia. We have further demonstrated that in isolated sympathetic neurons,  $\beta$ AR agonists elevate cAMP and activate PKA. The effects were more pronounced in neurons from pre-SHR rats. We also observed that  $\beta$ AR agonists enhanced  $[Ca^{2+}]_i$  in response to depolarization by high  $K^+$  in pre-SHR neurons only. In addition, we demonstrate the presence of mRNA and protein expression of PNMT, the enzyme involved in the synthesis of epinephrine in human and rat sympathetic stellate neurons. Moreover, we observed that epinephrine is present in diseased states and is actively released from prehypertensive, but not healthy rat neurons, suggesting preferential switching of neurotransmitter synthesis in disease.

Single or combinatorial administration of  $\beta$ -blockers is a mainstay treatment strategy for diseases caused by sympathetic overactivity, although the precise mechanisms that underpin the long-term beneficial effects are not entirely clear.<sup>12</sup> Current dogma suggests that the observed antihypertensive and cardioprotective effects of  $\beta$ -blockers are mediated through inhibition of cardiac and vascular  $\beta$ ARs, reducing myocardial work and total peripheral resistance.<sup>52</sup> Our findings suggest that the efficacy of clinical  $\beta$ -blockers may be attributed, at least in part, to a reduction in sympathetic hyperactivity and neurotransmission at the end-organ.

What is the cause for increased sympathetic neurotransmission before the onset of neurogenic hypertension? Emerging evidence suggests that impaired nitric oxide synthesis and reductions in cGMP–PKG (protein kinase G) signaling lead to pathological increases in  $[Ca^{2+}]_i$  and norepinephrine release at the end-organ.<sup>31,53</sup> Recently, we demonstrated that decreased cGMP signaling leads to enhanced N-type  $Ca^{2+}$  channel ( $Ca_v2.2$ ) currents and that this effect may be ameliorated by artificially increasing cytosolic cGMP.<sup>54,55</sup> cN signaling is acutely regulated by phosphodiesterase enzymes, and in early prehypertensive states, phosphodiesterase signaling is impaired, resulting in an imbalance between cAMP and cGMP signaling.<sup>54</sup> We, therefore, sought to ask the question, could high levels of neurotransmitter release act in an autocrine or paracrine fashion to increase neuronal cAMP and potentiate neurotransmission in a feed-forward manner?

Although it has been previously reported that presynaptic  $\beta$ ARs are present<sup>56</sup> and may be capable of facilitating norepinephrine release in several peripheral autonomic ganglia in rat, guinea pig, cat, rabbit, dog, and human<sup>13–17,19,57–62</sup>, the role of adrenergic signaling within the sympathetic stellate ganglia remains unclear, particularly in disease. In the present study, we confirmed the presence of both  $\beta_1$ AR and  $\beta_2$ AR isoforms in stellate ganglia from human and rat and found that activation of  $\beta$ ARs on rat sympathetic neuron led to a significantly greater increase in intracellular cAMP generation, PKA activity in pre-SHR compared with control neurons (Figure 2).

To assess whether  $\beta$ AR signaling facilitates cardiac-sympathetic neurotransmission,  $[Ca^{2+}]_i$  was measured in response to KCl in the absence or presence of isoprenaline. Consistent with the observed increases in  $\beta$ AR-mediated cAMP–PKA signaling in pre-SHR neurons, isoprenaline also increased KCl-evoked  $[Ca^{2+}]_i$  in prehypertensive states; whereas there was no effect of isoprenaline in control neurons (Figure 2E and 2F). These data demonstrate that enhanced  $\beta$ AR-mediated signaling in sympathetic neurons contributes to the  $Ca^{2+}$  phenotype and increases sympathetic transmission. Previous work has demonstrated that the N-type calcium channel is the primary voltage-gated channel responsible for  $Ca^{2+}$  influx in sympathetic neurons and carries a significantly larger  $Ca^{2+}$  current in pre-SHR and SHR neurons compared with controls.<sup>55,63</sup> N-type calcium channel activity is differentially regulated by PKA and PKG.<sup>54,55</sup> Therefore, we suggest that the isoprenaline-potentiated increases in  $[Ca^{2+}]_i$  in pre-SHR neurons primarily occurs as a result of  $\beta$ AR–cAMP activation that increases PKA-dependent phosphorylation of N-type calcium channel ( $Ca_v2.2$ ).

To establish whether the observed increases in cAMP–PKA activity occur downstream of  $\beta_1$ AR or  $\beta_2$ AR signaling, cells were perfused with selective agonists for either  $\beta_1$ AR or  $\beta_2$ AR subtypes in the presence of either alternate  $\beta$ AR antagonist. We found that selective activation of  $\beta_1$ AR or  $\beta_2$ AR led to significantly greater increases in cAMP in pre-SHR neurons compared with Wistar. Indeed, there was no measurable effect of  $\beta_1$ AR activation on [cAMP] in normotensive controls (Figure 3). Furthermore, stimulation of pre-SHR neurons with the  $\beta_2$ AR agonist salbutamol led to cAMP generation that was almost twice as high as  $\beta_1$ AR-evoked cAMP within pre-SHR neurons, suggesting a dominant role for  $\beta_2$ AR compared with  $\beta_1$ AR signaling. To establish whether increased  $\beta$ AR signaling in pre-SHR results from increases in  $\beta$ AR expression, we measured levels of  $\beta_1$ AR and  $\beta_2$ AR mRNA via qRT-PCR and RNAseq and quantified protein levels using sandwich ELISAs. Surprisingly, we observed that  $\beta$ AR transcripts and protein expression are reduced in pre-SHR stellates, as well as in aged SHR with established hypertension,<sup>6,29–31,33,35,36,42</sup> compared with age-matched Wistar neurons, in a similar manner to that reported in the myocardium.<sup>64,65</sup> We also report that in healthy ganglia,  $\beta_1$ AR expression decreases with age, much like in the heart (Figure 1). Together, these data suggest that in diseased states, the potentiating effects of  $\beta$ AR agonists may be mediated through impaired second messengers coupled to cAMP and its effector PKA, probably via impairment of phosphodiesterases to hydrolyze cAMP<sup>54,55</sup> rather than the G-protein coupled receptors themselves.

Which neurotransmitter preferentially activates presynaptic  $\beta$ ARs? Several studies suggest limited involvement of norepinephrine in potentiating presynaptic neurotransmission but argue for a critical role for epinephrine in enhancing release, particularly in patients with essential hypertension<sup>66</sup> or stress disorders.<sup>67,68</sup> The role of epinephrine in the pathogenesis of essential hypertension has been termed the Adrenaline Hypothesis<sup>23</sup>; however, the origins of local concentration of epinephrine remain unclear. Most reports suggest that high circulating plasma epinephrine concentrations



arise from the adrenal medulla with active reuptake into sympathetic nerve terminals.<sup>19,22,23,69–71</sup> Others have identified heightened epinephrine synthesis within the central nervous system, specifically the nucleus tractus solitarius<sup>72</sup> and hypothalamus<sup>72,73</sup> and suggest that this source of epinephrine may underpin the high plasma levels of epinephrine. Alternatively, some reports have identified *in situ* epinephrine synthesis within various sympathetic ganglia in rat and human, via a stress-inducible mechanism.<sup>19,24,66,72,74–77</sup> Our identification of PNMT mRNA and protein expression in human and rat cardiac-sympathetic ganglia (Figure 4) supports the findings of these earlier studies that epinephrine is synthesized in sympathetic stellate ganglia in disease.

What is the relevance of epinephrine synthesis in pre-hypertensive sympathetic stellate ganglia? The Adrenaline Hypothesis of hypertension proposes that stress and subsequent small incremental increases in epinephrine plays a major role in the pathogenesis of hypertension, not via epinephrine directly, but as a result of increased sympathetic activity and enhanced norepinephrine release.<sup>23</sup> This sustained increase in sympathetic activity caused by epinephrine leads to the development of hypertension. We have shown that epinephrine is synthesized in pre-SHR to a greater extent than in healthy sympathetic stellate ganglia and is only released from pre-SHR ganglia. Importantly, epinephrine has a 10-fold higher affinity for  $\beta_2$ AR than norepinephrine ( $EC_{50}$  5.2, 53.7 nmol/L, respectively) and is capable of generating 3× more cAMP than norepinephrine via  $\beta_2$ AR activation, a feature that may be mimicked by isoprenaline because of similarities in efficacy.<sup>78</sup> Subsequently, the high efficacy of epinephrine (and the relatively low efficacy of norepinephrine) at  $\beta_2$ AR has been shown to result in epinephrine-dependent norepinephrine transmission. Indeed, low concentrations of epinephrine (0.1–10 nmol/L) have been shown to be 100× to 500× more potent than norepinephrine in enhancing activity-dependent norepinephrine release.<sup>19,79–81</sup> Moreover, epinephrine may have a more sustained effect on norepinephrine release because of the extended tissue half-life of epinephrine.<sup>79</sup> Epinephrine-induced norepinephrine release has been identified in a wide variety of peripheral tissues in rat, rabbit, and human.<sup>18,19,22</sup>

We sought to investigate whether the presence of presynaptic PNMT plays a functional role in converting norepinephrine to epinephrine in rat stellate ganglia, by measuring total catecholamine content and electrically evoked catecholamines by high-pressure liquid chromatography coupled to electrochemical detection (Figure 5). We identified a significant decrease in total norepinephrine content in pre-SHR ganglia (74.8% of total catecholamine content) compared with norepinephrine calculated in Wistar ganglia (91.5% of total catecholamine content). We have also observed that the total content of epinephrine was significantly higher in pre-SHR ganglia (25.2% of total catecholamine content) compared with epinephrine levels quantified in Wistar ganglia (8.5% of total catecholamines measured). Furthermore, we found that on electric stimulation, the percentage ratio of norepinephrine:epinephrine released from Wistar ganglia was calculated as 91%:9%; whereas in pre-SHR ganglia, the ratio of catecholamines released

(norepinephrine:epinephrine) was 44%:56% (Figure 5), although the total amounts of catecholamines released during electric stimulation remained fairly similar between the strains ( $\approx 11$ –12 pg).

One recurrent feature in human and animal models of hypertension is the reduction in norepinephrine reuptake transport (NET), leading to larger and more sustained extracellular catecholamine concentrations.<sup>24,82–84</sup> Recently, it has been proposed that PNMT may also act as a DNA methylase, silencing NET transcription that may underpin the observed NET phenotype.<sup>24</sup> We have previously identified reductions in NET activity in the pre-SHR cardiac-stellate ganglia.<sup>82</sup>

## Limitations

In this study, we investigated the role and mechanisms involved in feed-forward presynaptic signaling in the cardiac-sympathetic ganglia. We performed a hypothesis neutral, nonbiased approach to sequencing the transcriptome of sympathetic stellate in adult rats that revealed the presence of RNA transcripts involved  $\beta$ AR receptor expression and epinephrine synthesis. We assessed the functional relevance of these findings by probing the adrenergic intracellular signaling pathways coupled to  $Ca^{2+}$ -mediated exocytosis. There were several limitations to these approaches. First, the stellate ganglion comprises a heterogeneous population of cell types. Indeed, we identified markers of fibroblasts and astrocytes, including vimentin and glial fibrillary acidic protein, respectively; however, we identified that a high number of transcripts were neuronal in phenotype. We also found that the subunit profile of nicotinic acetylcholine receptors matches those described for sympathetic neurons.<sup>85</sup> Moreover, immunocytochemistry highlighted the localization of  $\beta$ - and  $\alpha$ ARs on the soma and dendrites of TH-positive neurons. In support of these data, our collaborators have also identified the presence of transcripts encoding presynaptic  $\beta$ ARs in sorted sympathetic mouse neurons (Ana Domingos, personal communication, 2018). Second, in the absence of cardiac tracing experiments, we rely on anatomic literature,<sup>25–27</sup> and our own previous observations<sup>32,86–88</sup> that the results presented here are relevant to cardiac-sympathetic communication because significant myocardial sympathetic innervation has been shown to arise from the cervicothoracic ganglia. Third, we used stellates obtained from male rats. Although sex differences in hypertension and cardiovascular disease incidence have been widely reported,<sup>89</sup> in this study, we focused on investigating the transcriptome of the male rat stellate ganglia given that the prevalence for cardiovascular diseases is significantly higher in males than premenopausal women.<sup>89</sup> Fourth, cNs and phosphodiesterases reside in distinct subcellular compartments, and their localization with  $\beta$ ARs receptors is acutely regulated.<sup>90–92</sup> Similarly, the regulation of  $Ca^{2+}$  channels by PKA/PKG occurs in distinct signalosomes, conferring site-specific regulation of  $Ca^{2+}$  entry coupled to neurotransmission. Furthermore, the rate of phosphodiesterase hydrolysis is critically dependent on the concentration of both cAMP and cGMP that is reported to be different between cell types.<sup>93</sup> In this study, we measured global

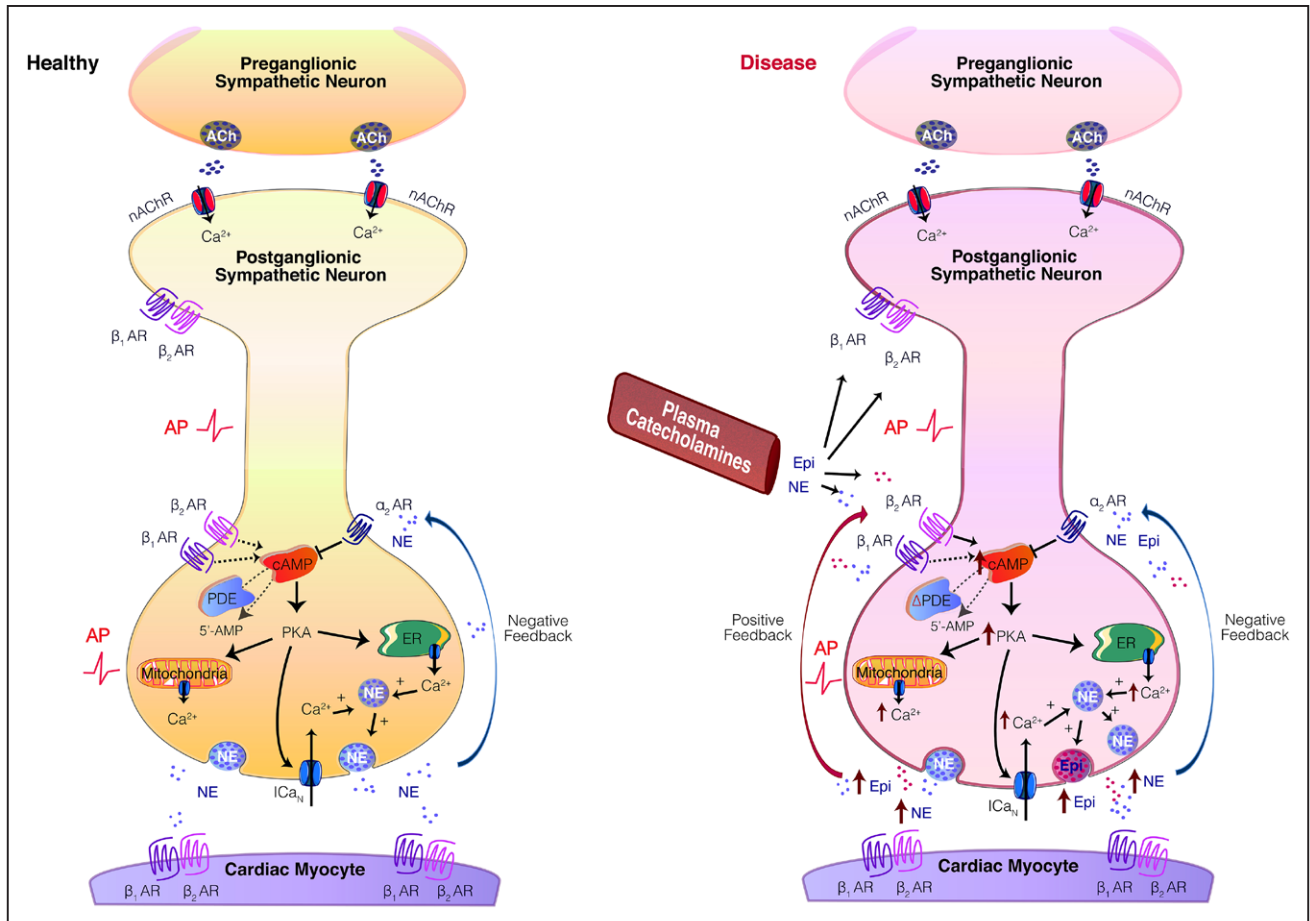


**Figure 6.** Model figure. The sympathetic stellate ganglia (cervicothoracic ganglia) are located alongside vertebrate T1 to T3. They are the primary sympathetic ganglia that innervate the heart and have been shown to exert the greatest control over increases in heart rate and contractility.<sup>25–28</sup> In healthy postganglionic sympathetic neurons (**A**),  $\text{Ca}^{2+}$ -dependent exocytosis facilitates the release of norepinephrine (NE) onto cardiac myocytes, where postsynaptic  $\beta_1$ - and  $\beta_2$ -adrenergic receptors (ARs) are activated. Increases in extracellular NE acts on presynaptic  $\alpha_2$ ARs, reducing adenyl cyclase (AC) activity through activation of inhibitory  $\text{G}\alpha_i$  G-proteins. Acute regulation of cAMP is maintained by phosphodiesterases (PDEs).<sup>90,91</sup> cAMP-dependent PKA (protein kinase A) activity increases intracellular  $\text{Ca}^{2+}$  ( $[\text{Ca}^{2+}]_i$ ) via phosphorylation of the N-type  $\text{Ca}^{2+}$  Channel ( $\text{ICa}_N$ ;  $\text{CaV2.2}$ )<sup>55</sup>; regulation of endoplasmic reticulum stores and mitochondrial  $\text{Ca}^{2+}$  release.<sup>31</sup> In neurons obtained from the prehypertensive SHR, a young genetic model of hypertension (**B**),  $\text{Ca}^{2+}$ -dependent exocytosis facilitates the release of NE and epinephrine (Epi). Activation of presynaptic  $\beta_2$ ARs in prehypertensive states<sup>29–36</sup> enhances cAMP generation, PKA activity, and  $[\text{Ca}^{2+}]_i$  to greater levels than in healthy neurons, facilitating neurotransmission in a potentiating feed-forward manner. This occurs preferentially via  $\beta_2$ AR activation. Catecholamines may also be supplied from the circulation. We propose that  $\beta$ -blockers may have efficacy at  $\beta$ ARs expressed on peripheral neurons, by reducing cardiac-sympathetic communication in hypertension and dysautonomias. ACh indicates acetylcholine; and nAChRs, nicotinic acetylcholine receptors.

cytosolic cAMP, PKA, and  $\text{Ca}^{2+}$  concentrations, therefore we cannot ascertain precisely where the key pathways converge. Site-specific FRET and  $\text{Ca}^{2+}$  sensors will be required to resolve the question of microdomain impairments in cN and effector signaling.

## Perspectives

Our data here demonstrate that in prehypertensive and hypertensive states, epinephrine is synthesized within presynaptic sympathetic nerve terminals and released on activation at the end-organ. In prehypertensive states, evoked release of epinephrine (that is exacerbated by decreased NET activity) may act preferentially on presynaptic  $\beta_2$ ARs to increase cAMP generation and PKA activity, thereby enhancing  $\text{Ca}^{2+}$  levels and neurotransmission in disease, in a manner akin to positive feedback. We suggest that epinephrine release at the end-organ may play a role in the

pathogenesis of hypertension. Figure 6 depicts the model signaling pathways in healthy and prehypertensive states and highlights potential sites for neural phenotypic targeting in disease. We suggest that in a model of early hypertension, activation of presynaptic  $\beta_2$ ARs enhances cAMP generation, PKA activity, and  $[\text{Ca}^{2+}]_i$  to greater levels than that measured in healthy neurons, facilitating both norepinephrine and epinephrine release. Presynaptic activation of  $\beta_2$ ARs (and  $\beta_1$ ARs to a lesser extent) further enhances neurotransmission in a potentiating feed-forward manner, with activation of  $\alpha_2$ ARs playing a role in negative feedback. Additional studies aimed at investigating the relative roles of epinephrine and norepinephrine in positive and negative feedbacks signaling may be of therapeutic relevance. Indeed, these findings may have implications beyond neurogenic hypertension and may offer benefit in other diseases of sympathetic overactivity, such as modulation of

renin–angiotensin–aldosterone release, chronic inflammatory diseases, and heart failure.

### Acknowledgments

We acknowledge the High-Throughput Genomics Group at the Wellcome Trust Centre for Human Genetics (funded by Wellcome Trust grant reference 090532/Z/09/Z) for the generation of the sequencing data. We acknowledge our collaborators Drs Ajijola, Shivkumar, and Ardell at the University of California, Los Angeles, Cardiac Arrhythmia Center for kindly extracting and shipping human sympathetic stellate ganglia from donor patients no. 19, no. 23, and no. 24. We thank Dr Threlfell in our department for her help and expertise with high-pressure liquid chromatography coupled to electrochemical detection experimental design and protocols. E.N. Bardsley and D.J. Paterson planned the project. E.N. Bardsley performed all of the rat and human RNA extraction, validation, and quantitative real-time polymerase chain reaction experiments. E.N. Bardsley performed all cell culturing and performed  $\text{Ca}^{2+}$  imaging, Förster resonance energy transfer imaging, ELISAs, and immunocytochemistry. K.J. Buckler assisted with the  $\text{Ca}^{2+}$  experiments. H. Davis performed the catecholamine high-pressure liquid chromatography coupled to electrochemical detection experiments. E.N. Bardsley analyzed all experimental data. E.N. Bardsley and H. Davis performed the RNA sequencing differential expression analysis. E.N. Bardsley and D.J. Paterson cowrote the paper. All authors edited the manuscript.

### Sources of Funding

This project was funded by the Wellcome Trust OXION initiative (105409/Z/14/Z), British Heart Foundation (BHF) Centre of Research Excellence and BHF (RG/17/14/33085), and National Institutes of Health SPARC (OT2OD023848) initiative.

### Disclosures

None.

### References

1. Florea VG, Cohn JN. The autonomic nervous system and heart failure. *Circ Res*. 2014;114:1815–1826. doi: 10.1161/CIRCRESAHA.114.302589.
2. Sprenger JU, Perera RK, Steinbrecher JH, Lehnart SE, Maier LS, Hasenfuss G, Nikolaev VO. In vivo model with targeted cAMP biosensor reveals changes in receptor-microdomain communication in cardiac disease. *Nat Commun*. 2015;6:6965. doi: 10.1038/ncomms7965.
3. Najafi A, Sequeira V, Kuster DW, van der Velden J.  $\beta$ -adrenergic receptor signalling and its functional consequences in the diseased heart. *Eur J Clin Invest*. 2016;46:362–374. doi: 10.1111/eci.12598.
4. Piccirillo G, Viola E, Nocco M, Durante M, Tarantini S, Marigliano V. Autonomic modulation of heart rate and blood pressure in normotensive offspring of hypertensive subjects. *J Lab Clin Med*. 2000;135:145–152. doi: 10.1067/mlc.2000.103428.
5. Lopes HF, Silva HB, Consolim-Colombo FM, Barreto Filho JA, Riccio GM, Giorgi DM, Krieger EM. Autonomic abnormalities demonstrable in young normotensive subjects who are children of hypertensive parents. *Braz J Med Biol Res*. 2000;33:51–54.
6. Thorén P, Ricksten SE. Recordings of renal and splanchnic sympathetic nervous activity in normotensive and spontaneously hypertensive rats. *Clin Sci (Lond)*. 1979;57(suppl 5):197s–199s.
7. Shanks J, Herring N. Peripheral cardiac sympathetic hyperactivity in cardiovascular disease: role of neuropeptides. *Am J Physiol Regul Integr Comp Physiol*. 2013;305:R1411–R1420. doi: 10.1152/ajpregu.00118.2013.
8. Li D, Paterson DJ. Cyclic nucleotide regulation of cardiac sympatho-vagal responsiveness. *J Physiol*. 2016;594:3993–4008. doi: 10.1113/JP271827.
9. Smith AA, Taylor T, Wortis SB. Abnormal catechol amine metabolism in familial dysautonomia. *N Engl J Med*. 1963;268:705–707. doi: 10.1056/NEJM196303282681304.
10. Wiysonge CS, Bradley HA, Volmink J, Mayosi BM, Opie LH. Beta-blockers for hypertension (review). *Cochrane Database Syst Rev*. 2017;1–93. doi: 10.1002/14651858.cd002003.pub5.
11. Frishman WH. Beta-adrenergic receptor blockers in hypertension: alive and well. *Prog Cardiovasc Dis*. 2016;59:247–252. doi: 10.1016/j.pcad.2016.10.005.
12. Wiysonge CS, Bradley HA, Volmink J, Mayosi BM. Cochrane corner: beta-blockers for hypertension. *Heart*. 2018;104:282–283. doi: 10.1136/heartjnl-2017-311585.
13. Adler-Graschinsky E, Langer SZ. Possible role of a beta-adrenoceptor in the regulation of noradrenaline release by nerve stimulation through a positive feed-back mechanism. *Br J Pharmacol*. 1975;53:43–50.
14. Nedergaard OA, Abrahamsen J. Modulation of noradrenaline release by activation of presynaptic beta-adrenoceptors in the cardiovascular system. *Ann NY Acad Sci*. 1990;604:528–544.
15. Apparsundaram S, Eikenburg DC. Role of prejunctional beta adrenoceptors in rat cardiac sympathetic neurotransmission. *J Pharmacol Exp Ther*. 1995;272:519–526.
16. Costa M, Majewski H. Facilitation of noradrenaline release from sympathetic nerves through activation of ACTH receptors, beta-adrenoceptors and angiotensin II receptors. *Br J Pharmacol*. 1988;95:993–1001.
17. Majewski H. Review modulation of noradrenaline release through activation of presynaptic beta-adrenoreceptors. *J Auton Pharmacol*. 1983;3:155–155. doi: 10.1111/j.1474-8673.1983.tb00529.x.
18. Lokhandwala MF, Eikenburg DC. Presynaptic receptors and alterations in norepinephrine release in spontaneously hypertensive rats. *Life Sci*. 1983;33:1527–1542.
19. Misu Y, Kubo T. Presynaptic beta-adrenoceptors. *Med Res Rev*. 1986;6:197–225.
20. Marrazzi AS. Electrical studies on the pharmacology of autonomic synapses ii. The action of a sympathomimetic drug (epinephrine) on sympathetic ganglia. *J Pharmacol Exp Ther*. 2006;65:395–404.
21. Goodall M, Kirshner N. Biosynthesis of epinephrine and norepinephrine by sympathetic nerves and ganglia. *Circulation*. 1958;17:366–371.
22. Floras JS. Epinephrine and the genesis of hypertension. *Hypertension*. 1992;19:1–18.
23. Brown MJ, Macquinn I. Is adrenaline the cause of essential hypertension? *Lancet*. 1981;2:1079–1082.
24. Esler M, Eikelis N, Schlaich M, Lambert G, Alvarenga M, Kaye D, El-Osta A, Guo L, Barton D, Pier C, Brechley C, Dawood T, Jennings G, Lambert E. Human sympathetic nerve biology: parallel influences of stress and epigenetics in essential hypertension and panic disorder. *Ann NY Acad Sci*. 2008;1148:338–348. doi: 10.1196/annals.1410.064.
25. Kawashima T. The autonomic nervous system of the human heart with special reference to its origin, course, and peripheral distribution. *Anat Embryol*. 2005;209:425–438. doi: 10.1007/s00429-005-0462-1.
26. Korzina MB, Korobkin AA, Vasilieva OA, Maslyukov PM. Morphological characteristics of the stellate ganglion in white rats. *Neurosci Behav Physiol*. 2011;41:436–439. doi: 10.1007/s11055-011-9433-6.
27. Ellison JP, Williams TH. Sympathetic nerve pathways to the human heart, and their variations. *Am J Anat*. 1969;124:149–162. doi: 10.1002/aja.1001240203.
28. Vaseghi M, Zhou W, Shi J, Ajijola OA, Hadaya J, Shivkumar K, Mahajan A. Sympathetic innervation of the anterior left ventricular wall by the right and left stellate ganglia. *Heart Rhythm*. 2012;9:1303–1309. doi: 10.1016/j.hrthm.2012.03.052.
29. Judy WV, Watanabe AM, Murphy WR, Aprison BS, Yu PL. Sympathetic nerve activity and blood pressure in normotensive backcross rats genetically related to the spontaneously hypertensive rat. *Hypertension*. 1979;1:598–604.
30. Dickhout JG, Lee RM. Blood pressure and heart rate development in young spontaneously hypertensive rats. *Am J Physiol*. 1998;274(3 pt 2):H794–H800.
31. Li D, Lee CW, Buckler K, Parekh A, Herring N, Paterson DJ. Abnormal intracellular calcium homeostasis in sympathetic neurons from young prehypertensive rats. *Hypertension*. 2012;59:642–649. doi: 10.1161/HYPERTENSIONAHA.111.186460.
32. Shanks J, Manou-Stathopoulou S, Lu CJ, Li D, Paterson DJ, Herring N. Cardiac sympathetic dysfunction in the prehypertensive spontaneously hypertensive rat. *Am J Physiol Heart Circ Physiol*. 2013;305:H980–H986. doi: 10.1152/ajpheart.00255.2013.
33. Heijnen BF, Van Essen H, Schalkwijk CG, Janssen BJ, Struijker-Boudier HA. Renal inflammatory markers during the onset of hypertension in spontaneously hypertensive rats. *Hypertens Res*. 2014;37:100–109. doi: 10.1038/hr.2013.99.
34. Komolova M, Friberg P, Adams MA. Altered vascular resistance properties and acute pressure-natriuresis mechanism in neonatal and weaning spontaneously hypertensive rats. *Hypertension*. 2012;59:979–984. doi: 10.1161/HYPERTENSIONAHA.111.178194.
35. Ely DL, Friberg P, Nilsson H, Folkow B. Blood pressure and heart rate responses to mental stress in spontaneously hypertensive (SHB) and



- normotensive (WKY) rats on various sodium diets. *Acta Physiol Scand*. 1985;123:159–169. doi: 10.1111/j.1748-1716.1985.tb07573.x.
36. Wilson AJ, Wang VY, Sands GB, Young AA, Nash MP, LeGrice IJ. Increased cardiac work provides a link between systemic hypertension and heart failure. *Physiol Rep*. 2017;5:e13104. doi: 10.14814/phy2.13104.
  37. Pijacka W, McBryde FD, Marvar PJ, Lincevicius GS, Abdala AP, Woodward L, Li D, Paterson DJ, Paton JF. Carotid sinus denervation ameliorates renovascular hypertension in adult Wistar rats. *J Physiol*. 2016;594:6255–6266. doi: 10.1111/JP272708.
  38. Oliveira-Sales EB, Colombari E, Abdala AP, Campos RR, Paton JF. Sympathetic overactivity occurs before hypertension in the two-kidney, one-clip model. *Exp Physiol*. 2016;101:67–80. doi: 10.1113/EP085390.
  39. Oliveira-Sales EB, Toward MA, Campos RR, Paton JF. Revealing the role of the autonomic nervous system in the development and maintenance of Goldblatt hypertension in rats. *Auton Neurosci*. 2014;183:23–29. doi: 10.1016/j.autneu.2014.02.001.
  40. Abdala AP, McBryde FD, Marina N, Hendy EB, Engelman ZJ, Fudim M, Sobotka PA, Gourine AV, Paton JF. Hypertension is critically dependent on the carotid body input in the spontaneously hypertensive rat. *J Physiol*. 2012;590:4269–4277. doi: 10.1113/jphysiol.2012.237800.
  41. Smith TL, Hutchins PM. Central hemodynamics in the developmental stage of spontaneous hypertension in the unanesthetized rat. *Hypertension*. 1979;1:508–517.
  42. Lee RM. Structural alterations of blood vessels in hypertensive rats. *Can J Physiol Pharmacol*. 1987;65:1528–1535.
  43. Conesa A, Madrigal P, Tarazona S, Gomez-Cabrero D, Cervera A, McPherson A, Szczeniński MW, Gaffney DJ, Elo LL, Zhang X, Mortazavi A. Erratum to: a survey of best practices for RNA-seq data analysis. *Genome Biol*. 2016;17:181. doi: 10.1186/s13059-016-1047-4.
  44. Hein L, Altman JD, Kobilka BK. Two functionally distinct  $\alpha$ 2-adrenergic receptors regulate sympathetic neurotransmission. *Nature*. 1999;402:181–184.
  45. Schmittgen TD, Livak KJ. Analyzing real-time PCR data by the comparative CT method. *Nat Protoc*. 2008;3:1101–1108. doi: 10.1038/nprot.2008.73.
  46. Klarenbeek J, Goedhart J, van Batenburg A, Groenewald D, Jalink K. Fourth-generation epac-based FRET sensors for cAMP feature exceptional brightness, photostability and dynamic range: characterization of dedicated sensors for FLIM, for ratiometry and with high affinity. *PLoS One*. 2015;10:e0122513. doi: 10.1371/journal.pone.0122513.
  47. Depry C, Allen MD, Zhang J. Visualization of PKA activity in plasma membrane microdomains. *Mol Biosyst*. 2011;7:52–58. doi: 10.1039/c0mb00079e.
  48. Williams RS, Bishop T. Selectivity of dobutamine for adrenergic receptor subtypes: in vitro analysis by radioligand binding. *J Clin Invest*. 1981;67:1703–1711.
  49. Baker JG. The selectivity of beta-adrenoceptor antagonists at the human beta1, beta2 and beta3 adrenoceptors. *Br J Pharmacol*. 2005;144:317–322. doi: 10.1038/sj.bjp.0706048.
  50. Cullum VA, Farmer JB, Jack D, Levy GP. Salbutamol: a new, selective beta-adrenoceptor receptor stimulant. *Br J Pharmacol*. 1969;35:141–151.
  51. Ladage D, Schwinger RH, Brixius K. Cardio-selective beta-blocker: pharmacological evidence and their influence on exercise capacity. *Cardiovasc Ther*. 2013;31:76–83. doi: 10.1111/j.1755-5922.2011.00306.x.
  52. Ram CVS. Beta-blockers in hypertension. *Am J Cardiol*. 2010;106:1819–1825. doi: 10.1016/j.amjcard.2010.08.023.
  53. Li D, Nikiforova N, Lu CJ, Wannop K, McMenamin M, Lee CW, Buckler KJ, Paterson DJ. Targeted neuronal nitric oxide synthase transgene delivery into stellate neurons reverses impaired intracellular calcium transients in prehypertensive rats. *Hypertension*. 2013;61:202–207. doi: 10.1161/HYPERTENSIONAHA.111.00105.
  54. Bardsley EN, Larsen HE, Paterson DJ. Impaired cAMP-cGMP cross-talk during cardiac sympathetic dysautonomia. *Channels (Austin)*. 2017;11:178–180. doi: 10.1080/19336950.2016.1259040.
  55. Larsen HE, Bardsley EN, Lefkimiatis K, Paterson DJ. Dysregulation of neuronal Ca2+ channel linked to heightened sympathetic phenotype in prohypertensive states. *J Neurosci*. 2016;36:8562–8573. doi: 10.1523/JNEUROSCI.1059-16.2016.
  56. Kazanietz MG, Enero MA. Role of cyclic AMP in the release of noradrenaline from isolated rat atria. Effect of pretreatment with clenbuterol. *Naunyn Schmiedeberg Arch Pharmacol*. 1992;346:311–314.
  57. Remie R, Knot HJ, Bos EA, Zaagsma J. Characterization of presynaptic beta-adrenoceptors facilitating endogenous noradrenaline release in the portal vein of permanently cannulated, freely moving rats. *Eur J Pharmacol*. 1988;157:37–43.
  58. Majewski H, Murphy TV. Beta-adrenoceptor blockade and sympathetic neurotransmission in the pithed rat. *J Hypertens*. 1989;7:991–996.
  59. Kazanietz MG, Enero MA. Modulation of noradrenaline release by presynaptic alpha-2 and beta adrenoceptors in rat atria. Effect of pretreatment with clenbuterol. *Naunyn Schmiedeberg Arch Pharmacol*. 1989;340:274–278.
  60. Tarizzo VI, Coppes RP, Dahlöf C, Zaagsma J. Pre- and postganglionic stimulation-induced noradrenaline overflow is markedly facilitated by a prejunctional beta 2-adrenoceptor-mediated control mechanism in the pithed rat. *Naunyn Schmiedeberg Arch Pharmacol*. 1994;349:570–577.
  61. Berg T.  $\beta$ 1-blockers lower norepinephrine release by inhibiting presynaptic, facilitating  $\beta$ 1-adrenoceptors in normotensive and hypertensive rats. *Front Neurol*. 2014;5:51. doi: 10.3389/fneur.2014.00051.
  62. Berg T. Altered  $\beta$ 1-3-adrenoceptor influence on  $\alpha$ 2-adrenoceptor-mediated control of catecholamine release and vascular tension in hypertensive rats. *Front Physiol*. 2015;6:120. doi: 10.3389/fphys.2015.00120.
  63. Tu H, Liu J, Zhang D, Zheng H, Patel KP, Cornish KG, Wang WZ, Muellemann RL, Li YL. Heart failure-induced changes of voltage-gated Ca2+ channels and cell excitability in rat cardiac postganglionic neurons. *Am J Physiol Cell Physiol*. 2014;306:C132–C142. doi: 10.1152/ajpcell.00223.2013.
  64. Blumenthal SJ, McConaughy MM, Iams SG. Myocardial adrenergic receptors and adenylate cyclase in the developing spontaneously hypertensive rat. *Clin Exp Hypertens A*. 1982;4:883–901.
  65. Madamanchi A. Beta-adrenergic receptor signaling in cardiac function and heart failure. *McGill J Med*. 2007;10:99–104.
  66. Rumanitir MS, Jennings GL, Lambert GW, Kaye DM, Seals DR, Esler MD. The 'adrenaline hypothesis' of hypertension revisited: evidence for adrenaline release from the heart of patients with essential hypertension. *J Hypertens*. 2000;18:717–723.
  67. Wilkinson DJ, Thompson JM, Lambert GW, Jennings GL, Schwarz RG, Jefferys D, Turner AG, Esler MD. Sympathetic activity in patients with panic disorder at rest, under laboratory mental stress, and during panic attacks. *Arch Gen Psychiatry*. 1998;55:511–520.
  68. Alvarenga ME, Richards JC, Lambert G, Esler MD. Psychophysiological mechanisms in panic disorder: a correlative analysis of noradrenaline spillover, neuronal noradrenaline reuptake, power spectral analysis of heart rate variability, and psychological variables. *Psychosom Med*. 2006;68:8–16. doi: 10.1097/01.psy.0000195872.00987.db.
  69. Majewski H, Hedler L, Starke K. The noradrenaline release rate in the anaesthetized rabbit: facilitation by adrenaline. *Naunyn Schmiedeberg Arch Pharmacol*. 1982;321:20–27. doi: 10.1007/BF00586343.
  70. Caramona MM, Soares-da-Silva P. The effects of chemical sympathectomy on dopamine, noradrenaline and adrenaline content in some peripheral tissues. *Br J Pharmacol*. 1985;86:351–356.
  71. Munch G, Nguyen NTB, Nekolla S, Ziegler S, Muzik O, Chakraborty P, Wieland DM, Schwaiger M. Evaluation of sympathetic nerve terminals with [ $^{11}\text{C}$ ]epinephrine and [ $^{11}\text{C}$ ]hydroxyephedrine and positron emission tomography. *Circulation*. 2000;101:516–523. doi: 10.1161/01.CIR.101.5.516.
  72. Gianutsos G, Moore KE. Epinephrine contents of sympathetic ganglia and brain regions of spontaneously hypertensive rats of different ages. *Proc Soc Exp Biol Med*. 1978;158:45–49.
  73. Torda C. Hypothalamic adrenaline synthesis after stimulation of the medial forebrain bundle. *Br J Pharmacol*. 1977;61:5–8.
  74. Kennedy B, Elayan H, Ziegler MG. Lung epinephrine synthesis. *Am J Physiol*. 1990;258(4 pt 1):L227–L231. doi: 10.1152/ajplung.1990.258.4.L227.
  75. Kubovcakova L, Micutkova L, Bartosova Z, Sabban EL, Krizanova O, Kvetnansky R. Identification of phenylethanolamine N-methyltransferase gene expression in stellate ganglia and its modulation by stress. *J Neurochem*. 2006;97:1419–1430. doi: 10.1111/j.1471-4159.2006.03832.x.
  76. Zeman M, Petrák J, Stebelová K, Nagy G, Krizanova O, Herichová I, Kvetnanský R. Endocrine rhythms and expression of selected genes in the brain, stellate ganglia, and adrenals of hypertensive TGR rats. *Ann NY Acad Sci*. 2008;1148:308–316. doi: 10.1196/annals.1410.069.
  77. Gavrilovic L, Spasojevic N, Varagic V, Dronjak S. Gene expression of catecholamine synthesizing enzymes in stellate ganglia of stressed rats. *Acta vet (Beogr)*. 2010;60:15–22. doi: 10.2298/avb1001015g.
  78. MacGregor DA, Prielipp RC, Butterworth JF, James RL, Royster RL. Relative efficacy and potency of  $\beta$ -adrenoceptor agonists for generating camp in human lymphocytes. *Chest*. 2016;109:194–200. doi: 10.1378/chest.109.1.194.



79. Majewski H, Rand MJ, Tung LH. Activation of prejunctional beta-adrenoceptors in rat atria by adrenaline applied exogenously or released as a co-transmitter. *Br J Pharmacol*. 1981;73:669–679.
80. Dahlöf C, Ljung B, Ablad B. Increased noradrenaline release in rat portal vein during sympathetic nerve stimulation due to activation of presynaptic beta-adrenoceptors by noradrenaline and adrenaline. *Eur J Pharmacol*. 1978;50:75–78.
81. Westfall TC, Peach MJ, Tittermary V. Enhancement of the electrically induced release of norepinephrine from the rat portal vein: mediation by beta 2-adrenoceptors. *Eur J Pharmacol*. 1979;58:67–74.
82. Shanks J, Mane S, Ryan R, Paterson DJ. Ganglion-specific impairment of the norepinephrine transporter in the hypertensive rat. *Hypertension*. 2013;61:187–193. doi: 10.1161/HYPERTENSIONAHA.112.202184.
83. Esler M, Rumantir M, Kaye D, Lambert G. The sympathetic neurobiology of essential hypertension: disparate influences of obesity, stress, and noradrenaline transporter dysfunction? *Am J Hypertens*. 2001;14(6 pt 2):139S–146S.
84. Kaye DM, Lambert GW, Lefkowitz J, Morris M, Jennings G, Esler MD. Neurochemical evidence of cardiac sympathetic activation and increased central nervous system norepinephrine turnover in severe congestive heart failure. *J Am Coll Cardiol*. 1994;23:570–578.
85. Leonard S, Bertrand D. Neuronal nicotinic receptors: from structure to function. *Nicotine Tob Res*. 2001;3:203–223. doi: 10.1080/14622200110050213.
86. Choate JK, Paterson DJ. Nitric oxide inhibits the positive chronotropic and inotropic responses to sympathetic nerve stimulation in the isolated guinea-pig atria. *J Auton Nerv Syst*. 1999;75:100–108.
87. Herring N, Lee CW, Sunderland N, Wright K, Paterson DJ. Pravastatin normalises peripheral cardiac sympathetic hyperactivity in the spontaneously hypertensive rat. *J Mol Cell Cardiol*. 2011;50:99–106. doi: 10.1016/j.yjmcc.2010.09.025.
88. Buttgeriet J, Shanks J, Li D, et al. C-type natriuretic peptide and natriuretic peptide receptor B signalling inhibits cardiac sympathetic neurotransmission and autonomic function. *Cardiovasc Res*. 2016;112:637–644. doi: 10.1093/cvr/cvw184.
89. Sandberg K, Ji H. Sex differences in primary hypertension. *Biol Sex Differ*. 2012;3:7. doi: 10.1186/2042-6410-3-7.
90. Stangherlin A, Zaccolo M. Phosphodiesterases and subcellular compartmentalized cAMP signaling in the cardiovascular system. *Am J Physiol Heart Circ Physiol*. 2012;302:H379–H390. doi: 10.1152/ajpheart.00766.2011.
91. Zaccolo M, Movsesian MA. cAMP and cGMP signaling cross-talk: role of phosphodiesterases and implications for cardiac pathophysiology. *Circ Res*. 2007;100:1569–1578. doi: 10.1161/CIRCRESAHA.106.144501.
92. Zoccarato A, Surdo NC, Aronsen JM, et al. Cardiac hypertrophy is inhibited by a local pool of cAMP regulated by phosphodiesterase 2. *Circ Res*. 2015;117:707–719. doi: 10.1161/CIRCRESAHA.114.305892.
93. Zhao CY, Greenstein JL, Winslow RL. Roles of phosphodiesterases in the regulation of the cardiac cyclic nucleotide cross-talk signaling network. *J Mol Cell Cardiol*. 2016;91:215–227. doi: 10.1016/j.yjmcc.2016.01.004.

## Novelty and Significance

### What Is New?

- We provide evidence for  $\beta_1$ - and  $\beta_2$ -adrenergic receptors in human stellate ganglia. These receptors are also conserved in rat stellates. We demonstrate that the cAMP–PKA signaling pathway coupled to activation of  $\beta$ -adrenergic receptors is impaired and exacerbates the  $\text{Ca}^{2+}$  phenotype in young prehypertensive rats.
- We have also shown that prehypertensive rat stellate neurons synthesize and release epinephrine.

### What Is Relevant?

- Neurotransmitter switching to epinephrine may be an early cellular marker because this neurochemical phenotype may reflect sympathetic impairment in the early stages of disease progression.
- Targeting the  $\beta$ -adrenergic intracellular signaling pathway and reducing PNMT (phenylethanolamine-N-methyltransferase) activity may be therapeutically relevant for the early treatment of sympathetic dysautonomia.

### Summary

Using a combination of RNA sequencing, quantitative real-time polymerase chain reaction, immunocytochemistry, ELISA, Förster resonance energy transfer and  $\text{Ca}^{2+}$  imaging, we have shown the presence  $\beta$ -adrenergic receptors on presynaptic sympathetic neurons in human and rat. We have demonstrated that catecholaminergic stimulation of these receptors exacerbates the sympathetic  $\text{Ca}^{2+}$  phenotype in the pre-SHR before the onset of hypertension. Using high-pressure liquid chromatography coupled to electrochemical detection, we have also found that physiological concentrations of epinephrine are released from sympathetic ganglia before increases in blood pressure occur. This may reflect a site of neural impairment in disease progression.

## Neurotransmitter Switching Coupled to $\beta$ -Adrenergic Signaling in Sympathetic Neurons in Prehypertensive States

Emma N. Bardsley, Harvey Davis, Keith J. Buckler and David J. Paterson

*Hypertension*. 2018;71:1226-1238; originally published online April 23, 2018;

doi: 10.1161/HYPERTENSIONAHA.118.10844

*Hypertension* is published by the American Heart Association, 7272 Greenville Avenue, Dallas, TX 75231

Copyright © 2018 American Heart Association, Inc. All rights reserved.

Print ISSN: 0194-911X. Online ISSN: 1524-4563

The online version of this article, along with updated information and services, is located on the World Wide Web at:

<http://hyper.ahajournals.org/content/71/6/1226>

Free via Open Access

Data Supplement (unedited) at:

<http://hyper.ahajournals.org/content/suppl/2018/04/20/HYPERTENSIONAHA.118.10844.DC1>

**Permissions:** Requests for permissions to reproduce figures, tables, or portions of articles originally published in *Hypertension* can be obtained via RightsLink, a service of the Copyright Clearance Center, not the Editorial Office. Once the online version of the published article for which permission is being requested is located, click Request Permissions in the middle column of the Web page under Services. Further information about this process is available in the [Permissions and Rights Question and Answer](#) document.

**Reprints:** Information about reprints can be found online at:

<http://www.lww.com/reprints>

**Subscriptions:** Information about subscribing to *Hypertension* is online at:

<http://hyper.ahajournals.org/subscriptions/>

## ONLINE SUPPLEMENT

### NEUROTRANSMITTER SWITCHING COUPLED TO BETA-ADRENERGIC SIGNALING IN SYMPATHETIC NEURONS IN PREHYPERTENSIVE STATES

Emma N. Bardsley\*<sup>1</sup>, Harvey Davis<sup>1</sup>, Keith J. Buckler<sup>1</sup>, David J. Paterson\*<sup>1</sup>

<sup>1</sup>Wellcome Trust OXION Initiative in Ion Channels and Disease, Burdon Sanderson Cardiac Science Centre, Department of Physiology, Anatomy and Genetics, Sherrington Building, University of Oxford, Oxford, OX1 3PT, UK

\*Corresponding Authors: Miss Emma Nicole Bardsley, University of Oxford, Department of Physiology, Anatomy and Genetics, Oxford, OX1 3PT, UK; [emma.bardsley@dpag.ox.ac.uk](mailto:emma.bardsley@dpag.ox.ac.uk), tel. +44 (0)1865 272471.

Prof. David James Paterson, University of Oxford, Department of Physiology, Anatomy and Genetics, Oxford, OX1 3PT, UK; [david.paterson@dpag.ox.ac.uk](mailto:david.paterson@dpag.ox.ac.uk), tel. +44 (0)1865 272471.

Short title: **Neurotransmitter Switch in Prehypertension**

### Supplemental Materials and Methods

**Reagents.** All drugs and reagents were sourced from Sigma-Aldrich UK unless otherwise stated.

**Adenovirus generation.** The cAMP-sensitive FRET sensor Epacs1-H187 (EpacH187) and the PKA-sensitive FRET sensor AKAR4 were obtained as described previously<sup>1</sup>. Generation and amplification of the virus particles was outsourced to Vector Biolabs.

**Neuronal Isolation from Rat Sympathetic Cardiac Ganglia.** Rats were anaesthetized in an induction chamber (3-5% isoflurane) and humanely killed by a Home Office approved Schedule 1 method: overdose of pentobarbital (Euthatal, 200 mg/mL) and exsanguination. The stellate ganglia were removed, de-sheathed from connective tissue, dissected and enzymatically digested with collagenase (type IV, 1 mg/mL, 37 °C) and trypsin (type I, 1 mg/mL, 37 °C). Stellates were washed with a modified L-15 blocking medium that was equilibrated prior to use (37 °C, 5 % CO<sub>2</sub>) and the ganglia were dissociated into a single-cell suspension via manual trituration in pre-equilibrated plating medium (37 °C, 5 % CO<sub>2</sub>). Post-ganglionic sympathetic neurons (PGSNs) were plated on Poly-D-Lysine/laminin-coated coverslips (6 mm, VWR International) and incubated in plating medium (37 °C, 5 % CO<sub>2</sub>) until required for use.

**Immunocytochemistry.** PGSNs were cultured from 3-5-week pre-SHR and Wistar control rats. Stellate neurons were fixed with paraformaldehyde (2%, 5 mins) before blocking and permeablizing with goat serum (10%), bovine serum albumin (0.3%) and Triton X-100 (0.1%) in dPBS without Ca<sup>2+</sup> and Mg<sup>2+</sup> (1-hour, room temperature (RT)). Cells were washed thoroughly with dPBS (3 x 10 min) and incubated in primary antibodies (1-hour, 37 °C). The following antibodies were used: anti-tyrosine hydroxylase (TH, 1:250, T1299, Abcam), anti-β<sub>1</sub>AR (ab3442, 1:100, Abcam), anti-β<sub>2</sub>AR, (ab182136, 1:200, Abcam). Cells were incubated with the appropriate secondary antibodies (Alexa Fluor, 1:1000, 2 hours, 37 °C) before they were mounted on microscope slides using medium containing DAPI (Vectashield, Vector Laboratories) and sealed. Control experiments that were carried out in the absence of primary antibodies did not display any fluorescence except DAPI, confirming the absence of non-specific binding. Specificity of primary antibodies for β<sub>1</sub>AR and β<sub>2</sub>AR was also validated via Western blotting (data not shown). Cells were imaged using 40X or 60X objectives on a confocal microscope (Live Cell Olympus Inverted Confocal or Zeiss LSM 880 Airy Scan Upright Confocal). Z-stack images were edited and cell sizes were measured using Fiji software (ImageJ)<sup>2,3</sup>.

**RNA Extraction from Sympathetic Cardiac Ganglia for RNA Sequencing and qRT-PCR.** Left and right PGSNs were dissected from 16-week-old male SHR and age-matched male Wistar rats. Briefly, rats were anaesthetized in an induction chamber (3-5% isoflurane) and humanely killed by a Home Office approved Schedule 1 method: overdose of pentobarbital (Euthatal, 200 mg/mL) and exsanguination. Right stellate ganglia were removed for RNA sequencing and the left stellate ganglia were used for matched qRT-PCR experiments. Stellate ganglia were placed in Hanks Buffered Saline Solution without Ca<sup>2+</sup> and Mg<sup>2+</sup>. For clinical samples, human stellate ganglia were kindly sent by Drs Ajijola, Ardell and Shivkumar



## Online Supplement: Neurotransmitter Switch in Prehypertension

from UCLA Cardiac Arrhythmia Center and shipped on dry ice in RNeasy<sup>®</sup> RNA Stabilization Solution (ThermoFisher). Rat and human ganglia were cleaned and de-sheathed. Each ganglion was transferred immediately to RLT lysis buffer (Qiagen) with  $\beta$ -mercaptoethanol (1%), and each sample contained tissue from one stellate. Rat stellates were finely chopped and carefully triturated with fire-blown Pasteur pipettes until adequately digested. Human stellates were manually homogenized. RNA was extracted using an RNeasy Mini RNA Extraction Kit (Qiagen) and human RNA was extracted using an RNeasy Maxi RNA Extraction Kit (Qiagen) in accordance with the manufacturer's instructions. RNA samples were aliquoted for qRT PCR and quality control experiments, snap frozen in liquid nitrogen and stored at -80 °C. The RNA quality and integrity from each sample, was confirmed using a 2100 Bioanalyzer Instrument with an RNA picochip (Agilent). Rat samples with an RNA Integrity Number (RIN) less than 8.5 were discarded. Due to difficulties with fast shipping of human samples we accepted human RNA samples with RINs above 5.7. RNA concentrations were determined using a Qubit RNA High Sensitivity Assay Kit (Molecular Probes, Life Technologies) and a Qubit<sup>®</sup> 2.0 Fluorometer (Invitrogen, Life Technologies).

***cDNA library preparation for RNA Sequencing.*** Four replicate samples containing total RNA extracted from the right sympathetic stellate ganglion of 16-week-old male SHR (n=4) and age-matched Wistar (n=4) were sent to the High-Throughput Genomics Group at the Wellcome Trust Centre for Human Genetics (WTCHG) for RNAseq library construction and sequencing using an Illumina HiSeq 4000 (Illumina, Inc., San Diego, USA). The sequencing libraries were amplified using a SMARTer (first strand synthesis) amplification protocol due to the low initial RNA concentrations obtained from a single stellate and prepared for paired-end sequencing (2 x 75 bp). Each sample was sequenced on two separate lanes to minimize technical error and to increase the sequencing depth (~15-25 million reads per lane). Samples were randomized and blinded to the experimenter. The number of replicates and the sequencing parameters established, were based on recommendations from WTCHG and those published by Conesa et al., 2016<sup>2</sup>.

***Quasi-mapping.*** Transcripts were quantified via the Salmon (version 0.8.2) package using the transcriptome-based quasi-mapping mode<sup>3</sup>. The following commands were used for quasi-mapping in accordance with the Salmon guidelines:

```
salmon quant -l transcripts_index -l ISR a -1 /SampleX_lane1_mate1.fastq.gz /  
SampleX_lane2_mate1.fastq.gz -2 / SampleX_lane1_mate2.fastq.gz /  
SampleX_lane2_mate2.fastq.gz -o Sample1 --dumpEq --posBias --gcBias --  
writeUnmappedNames. The transcript index used during quasi-mapping was derived from  
the UCSC refseq rn6.0 mRNA library available at the following link:  
http://hgdownload.soe.ucsc.edu/goldenPath/rn6/bigZips/refMrna.fa.gz.
```

Data files were assigned alternative names to blind the experimenter during the relevant stages of the quasi-mapping analysis.

***RNAseq Differential Expression Analysis.*** Following sample quantification, the data were imported into R and summarized at the gene-level using the 'Tximport' function (v1.4.0)<sup>4</sup>. A differential expression analysis of the gene counts for Wistar and SHR samples was performed using the 'DESeq2' command in the R package DESeq2 (version 1.16.1)<sup>4</sup>. Significance for differential expression was accepted at the Benjamini-Hochberg adjusted

## Online Supplement: Neurotransmitter Switch in Prehypertension

value  $p < 0.05$ . The 'LFCshrink' function was used to shrink  $\log_2$  fold change after analysis, for visualization and ranking of genes, as per the DESeq2 vignette<sup>4</sup>.

**cDNA Library Preparation for qRT-PCR.** 50 ng stellate RNA was obtained for constructing qRT-PCR cDNA libraries ( $n=4/\text{group}$ ). For conversion of rat PGSN RNA, the SuperScript™ III VILO™ cDNA synthesis protocol was followed according to manufacturer's instructions. For conversion of human PGSN RNA, the SuperScript™ IV VILO™ cDNA synthesis protocol was followed according to manufacturer's instructions (ThermoFisher). The concentration of cDNA in each sample and the 260/280 ratios were calculated (NanoDrop Lite) to detect the presence of contaminants. cDNA samples with an abnormal 260/280 ratio ( $<1.7$  and  $>1.95$ ) were discarded. The cDNA samples were aliquoted and numerically labelled to blind the experimenter to the rat strain during experimentation. Samples were frozen at  $-80^\circ\text{C}$  for long-term storage or retained at  $4^\circ\text{C}$  for immediate use.

**Two-Step Quantitative Real-Time Polymerase Chain Reaction.** qRT-PCR was used to confirm the presence of the following mRNA transcripts in the PGSN cDNA libraries:  $\beta_1\text{AR}$  (Adrb1; Rn00824536\_s1, Hs02330048\_s1; rat, human respectively),  $\beta_2\text{AR}$  (Adrb2; Rn00560650\_s1, Hs00240532\_s1; rat, human),  $\alpha_2\text{aAR}$  (Adra2a; Rn00562488\_s1, Hs01099503\_s1); PAH (Pah; Rn00561708\_m1, rat), TH (Th; Rn00562500\_m1, Hs01002182\_m1; rat, human), DDC (Ddc; Rn01401189\_m1, rat), DBH (Dbh; Rn00565819\_m1, rat), PNMT (Pnmt; Rn01495589\_g1, Hs01557113\_g1; rat, human respectively). The following controls were selected: beta-2-microglobulin (B2m; Rn00560865\_m1, Hs00187842\_m1; rat, human), glyceraldehyde-3-phosphate dehydrogenase (Gapdh; Rn99999916\_s1, Hs02786624\_g1; rat, human). TaqMan® Gene Expression Master Mix (ThermoFisher) was added to each cDNA sample in addition to the selected primer conjugated to a FAM dye and nuclease-free  $\text{H}_2\text{O}$ . cDNA samples or control samples with no reverse transcriptase were diluted 1:20 for optimal PCR reactions. 20  $\mu\text{L}$  samples (3 repeats) were added to a 96-well plate and run on a real-time quantitative PCR thermocycler (ABI, PRISM). Temperatures were held at  $50^\circ\text{C}$  (2 min) and  $95^\circ\text{C}$  (10 min) before thermal cycling (40 cycles) under the following conditions  $95^\circ\text{C}$  (15 s),  $60^\circ\text{C}$  (1 min). Data displayed in the results section depicts gene counts normalised to B2m; however, each primer was analysed against two housekeeping genes, B2m and Gapdh for validation and accuracy of qRT-PCR data. The relative amount of each transcript was calculated using the comparative ( $C_T$ ) method ( $\Delta\Delta C_T$ , rat;  $\Delta C_T$ , human)<sup>5</sup>.

**Quantitative Enzyme Linked Immunosorbent Assay (ELISA).** Protein was extracted from stellate ganglia obtained from 4-week and 20-week male SHR, age-matched Wistar rats and human donors. 100 mg of rat stellate tissue was pooled and homogenized in ice-cold dPBS without  $\text{Ca}^{2+}$  or  $\text{Mg}^{2+}$ . In alternative experiments, tissue from three human ganglia (80 mg) was separately homogenized in ice-cold dPBS without  $\text{Ca}^{2+}$  or  $\text{Mg}^{2+}$ . The protein concentration in each sample was quantified using a protein assay (BioRad DC) as per manufacturer's instructions and the total protein concentration in each sample was normalized. Protein concentrations were established using sandwich ELISAs for  $\beta_1\text{AR}$  (CSB-EL001391RA, CSB-EL001391HU; rat, human respectively),  $\beta_2\text{AR}$  (CSB-EL001392RA, CSB-EL001392HU; rat, human respectively), PNMT (CSB-EL018274RA, CSB-EL018274HU; PNMT rat, human respectively) and TH (CSB-E13102r, CSB-E09661h; rat, human respectively). ELISA assays were performed in accordance with the manufacturer's instructions (CUSABIO,

## Online Supplement: Neurotransmitter Switch in Prehypertension

USA). Background absorbance was measured at 540 nm and subtracted from the values obtained at 450 nm (Infinite F500, TECAN). Absolute concentrations of protein were quantified using a standard curve generated from the supplied standards.

**Live-Cell Förster Resonance Energy Transfer (FRET) Microscopy.** FRET was employed to monitor real-time changes in intracellular cAMP generation and protein kinase (PKA) activity in randomly selected PGSNs obtained from 4-week pre-SHR and Wistar rats. Stellate neurons were cultured and transduced with adenovirus particles encoding the respective FRET biosensors Epacs1H187:  $5.1 \times 10^8$  PFU / mL, AKAR4:  $1.3 \times 10^9$  PFU / mL) for 24 hours. Experiments were blinded wherever possible, however due to the comprehensive 3-4-day culturing/imaging protocol, it was not possible for a single experimenter to be blinded during the imaging experiments. To detect dynamic changes in cytosolic cAMP or PKA activity, cells were transduced with the loss-of-FRET sensor Epacs1H187<sup>6</sup> or the gain-of-FRET biosensor A Kinase Activity Reporter 4 (AKAR4)<sup>7</sup> respectively. FRET biosensor-expressing neurons were imaged 3-4 days post-culture, on an inverted microscope (Nikon) connected to an OptoLED fluorescence imaging system (Cairn Research Ltd., UK). Cells were imaged using 40X or 60X oil-immersion objectives and images were captured with a CoolSNAP HQ2 digital CCD camera (Photometrics). A beam splitter (DV2 Photometrics) included the emission filters for CFP and YFP (ET480/30M, ET535/40M) respectively, and a dichroic mirror (505DCXR). The cells were excited at 430 nm for 100 ms every 15 s. CFP and YFP emission intensities were measured at 480 nm and 535 nm were acquired using Optofluor software (Cairn Research Ltd., UK). For the Epacs1H187 loss-of-FRET sensor, CFP / YFP ratios were calculated. For AKAR4, a gain-of-FRET sensor, YFP / CFP emission intensity ratios were calculated. Background fluorescence was subtracted from emission intensity ratios and data were expressed as intensity per unit time. Mean FRET responses were expressed as the percentage change from baseline ( $\Delta R/R_0$  where  $\Delta R = R - R_0$ .  $R_0$  is the mean ratio over 30 s at baseline in the absence of drug, and  $R$  is the mean ratio calculated over 30 s in the presence of drug treatment).

During FRET experiments, cells were perfused continuously with Tyrode's solution via a gravity-fed perfusion system and the flow rate was controlled at 2-3 mL/min. A stable baseline of at least 2 minutes was required at the start of each experiment. Pharmacological compounds were diluted in Tyrode solution and perfused at the following concentrations: isoprenaline (ISO) 10 nmol/L to 10  $\mu$ mol/L;  $\beta_1$ AR agonist dobutamine (DOB) 50  $\mu$ mol/L;  $\beta_1$ AR antagonist metoprolol, 100 nmol/L to 10  $\mu$ mol/L;  $\beta_2$ AR agonist salbutamol (SAL), 10  $\mu$ mol/L;  $\beta_2$ AR agonist ICI 118,551 10 nmol/L to 10  $\mu$ mol/L. In all experiments, the maximal FRET change of each cell was recorded by exposing the cells to saturating concentrations of an adenylyl cyclase (AC) activator forskolin (FSK) 25  $\mu$ mol/L and a non-specific PDE inhibitor 3-isobutyl 1-methylxanthine (IBMX) 100  $\mu$ mol/L, to ensure that the cells responded similarly to the biosensors. In the absence of a FSK/IBMX response, cells were excluded from analysis. The number of cells per group were based on previously-calculated power analyses. For comparisons between cells, the average percentage FRET change was calculated over a 30 s period once equilibrium was established.

**Real-Time Calcium Measurements.** PGSNs from 4-week pre-SHR and Wistar rats were dissected, dissociated and incubated for 4-6 hours on the day of culture until they fully adhered to Poly-D-Lysine / laminin-coated coverslips (37°C, 5% CO<sub>2</sub>). To investigate Ca<sup>2+</sup>

## Online Supplement: Neurotransmitter Switch in Prehypertension

responses to ISO, neurons from 4-week Wistar and pre-SHR were incubated in Indo-1 acetoxymethyl ester (Indo-1AM, ThermoFisher; 2  $\mu\text{mol/L}$ , 45 mins, RT). Stellate neurons loaded with Indo-1AM were imaged on an inverted Nikon Diaphot 200 microscope (Nikon, Tokyo, Japan) and excited at 340 nm with a 100 W Xenon lamp (Nikon, Tokyo, Japan). The emission was split by a dichroic mirror (450 nm) and fluorescence was detected at 405 nm (calcium bound) and 495 nm (calcium free) by two tri-alkali photomultiplier tubes (PMTs, ET Enterprises Ltd., UK) each housed in air cooled enclosures (FACT50, ET Enterprises Ltd., UK) to maintain PMT temperatures at -20 °C. The output from each PMT was integrated in a current-to-voltage converter and digitized at a sampling frequency of 250 Hz (CED 1401). Signals at 405 nm and 495 nm were acquired with Spike2 software and automatically converted into a ratio (495 nm / 405 nm). Recorded values were averaged over 0.5 s intervals providing a final sampling rate of 2 Hz.

During  $\text{Ca}^{2+}$  imaging experiments a stable baseline was recorded for 30 s prior to stimulation. PGSNs were subsequently stimulated with 50 mmol/L KCl in  $\text{CO}_2$  /  $\text{HCO}_3$  buffered Tyrode solution with an equimolar reduction in NaCl. Upon return to baseline, cells were perfused with isoprenaline (ISO, 1  $\mu\text{mol/L}$ ) for 4 minutes and re-stimulated with 50 mmol/L  $\text{K}^+$  in the presence of ISO (1  $\mu\text{mol/L}$ ). For control experiments, no ISO was administered. In the absence of a KCl response, cells were excluded from analysis. The values obtained from the  $\text{Ca}^{2+}$  peak following each KCl stimulation were averaged and baseline values were subtracted from absolute peak size. To determine the effect of the compound on KCl-evoked  $[\text{Ca}^{2+}]_i$ ; the ratio 'S2 / S1' was calculated, where S2 was the stimulus in the presence of drug and S1 was the stimulus prior to drug administration. Ratios were compared to time-controlled experiments, where S1 and S2 were both recorded in the absence of drug. Ratiometric data were obtained through conversion of raw data sheets into text files. Fluorescence values were transformed to  $[\text{Ca}^{2+}]_i$  concentrations using the following equation derived by Grynkiewicz et al.,<sup>8</sup>:

$$[\text{Ca}^{2+}]_i = Kd \times \left\{ \frac{sf}{sb} \right\} \times \left\{ \frac{(R - R_{min})}{(R_{max} - R)} \right\}$$

For control experiments measuring intracellular  $\text{Ca}^{2+}$ , Wistar and WKY neurons were cultured and grown on Poly-D-lysine/laminin-coated coverslips (6 mm, VWR International) and incubated in plating medium (37 °C, 5 %  $\text{CO}_2$ ) for 36-48 hours. Prior to imaging, cells were incubated in plating media with the ratiometric  $\text{Ca}^{2+}$  dye Fura-2AM (ThermoFisher; 2  $\mu\text{mol/L}$ , 45 mins, RT). Calcium concentrations were measured at baseline (Tyrode's, 37 °C) and in response to a KCl challenge (50 mmol/L, equimolar reduction in NaCl, 37 °C). Fura-2AM was excited at 340/380 nm at an interval of 3500 ms. The emitted fluorescence was calculated at 510 nm and converted to  $\text{Ca}^{2+}$  concentrations using the Grynkiewicz equation as described<sup>8</sup>.

**High-Pressure Liquid Chromatography Coupled to Electrochemical Detection (HPLC-EC).** To investigate concentrations of norepinephrine (NE) or epinephrine (Epi) in pre-SHR compared with Wistar stellates, whole fresh ganglia were dissected from 4-week pre-SHR (n=4 rats) and 4-week Wistar (n=8 rats). For each experiment, a single ganglion was cleaned, de-sheathed and allowed to recover in bicarbonate-buffered carbogenated Tyrode's solution (5 min, 37 °C, 95 %  $\text{O}_2$  / 5 %  $\text{CO}_2$ ). The ganglia were subsequently incubated in bicarbonate-



## Online Supplement: Neurotransmitter Switch in Prehypertension

buffered Tyrode's containing the NET-reuptake inhibitor, desipramine (1  $\mu\text{mol/L}$ , 10 min, 37  $^{\circ}\text{C}$ ). Ganglia were electrically stimulated (3 mA, 5 Hz, 5 min); parameters that were adapted from previous electrical stimulation methods<sup>9</sup>. The perfusate was removed and perchloric acid (PCA, 0.1 mol/L) was added at each step to prevent the oxidation of catecholamines. Samples were kept on ice before freezing at -80  $^{\circ}\text{C}$ . At the end of each experiment, whole stellate ganglia were homogenized in bicarbonate-buffered Tyrode's solution containing PCA (0.1 mol/L), centrifuged (15,000 G, 15 min, 4  $^{\circ}\text{C}$ ) and the supernatant stored at -80  $^{\circ}\text{C}$ . For detection and quantification of NE and Epi, the samples were randomized, loaded into an autosampler (JASCO, Model AS-2055/2057) and detected with an isocratic HPLC system. HPLC separation was performed at the flow rate 1 mL / min using a C18 reverse-phase column (CP30710 Microsorb 100-5 C18 S250 x4.6mm, Agilent). The mobile phase (pH 4.7) comprised methanol (11.5% v/v),  $\text{NaH}_2\text{PO}_4$  (120 mmol/L), EDTA (0.8 mmol/L), and sodium octane sulfonate (OSA, 0.5 mmol/L). Concentrations of NE and Epi were quantified using an LC-4B electrochemical detector and a carbon working electrode maintained at +0.7 V versus an Ag/AgCl reference electrode (Decade SDC, Antec). Chromatogram peaks were quantified (area under curve; CLARITY software) and the concentrations of NE were calculated against a 50 mg standard of NE and Epi dissolved in bicarbonate-buffered Tyrode's containing PCA (0.1 mol/L). In the absence of any NA detection, cells were excluded from analysis.

**Statistical Analysis.** Data were analyzed using GraphPad Prism software (v6/7). When the data passed normality tests (D'Agostino-Pearson omnibus test or Shapiro-Wilk<sup>10</sup>) unpaired two-tailed Student t-tests, or a one or two-way analysis of variance (ANOVA) were used. When the data were not normally distributed, the appropriate nonparametric tests were used with the specific statistical test reported in the figure legend. All data are expressed as the mean  $\pm$  SEM. Statistical significance was accepted at  $p < 0.05$  unless otherwise described.

### Supplementary References

1. Larsen HE, Bardsley EN, Lefkimiatis K, Paterson DJ. Dysregulation of neuronal  $\text{Ca}^{2+}$  channel linked to heightened sympathetic phenotype in prohypertensive states. *J Neurosci*. 2016;36(33):8562-8573. doi:10.1523/JNEUROSCI.1059-16.2016.
2. Conesa A, Madrigal P, Tarazona S, Gomez-Cabrero D, Cervera A, McPherson A, Szczesniak MW, Gaffney DJ, Elo LL, Zhang X, Mortazavi A. A survey of best practices for RNA-seq data analysis. *Genome Biol*. 2016:1-19. doi:10.1186/s13059-016-0881-8.
3. Patro R, Duggal G, Love MI, Irizarry RA, Kingsford C. Salmon provides fast and bias-aware quantification of transcript expression. *Nat Methods*. 2017;14(4):417-419. doi:10.1038/nmeth.4197.
4. Love MI, Huber W, Anders S. Moderated estimation of fold change and dispersion for RNA-seq data with DESeq2. *Genome Biol*. 2014;15(12):31-62. doi:10.1186/s13059-014-0550-8.
5. Schmittgen TD, Livak KJ. Analyzing real-time PCR data by the comparative CT method. *Nat Protoc*. 2008;3(6):1101-1108. doi:10.1038/nprot.2008.73.
6. Klarenbeek J, Goedhart J, van Batenburg A, Groenewald D, Jalink K. Fourth-generation Epac-based FRET sensors for cAMP feature exceptional brightness, photostability and dynamic range: characterization of dedicated sensors for FLIM, for ratiometry and with high affinity. Anderson KI, ed. *PLoS ONE*. 2015;10(4):1-11. doi:10.1371/journal.pone.0122513.
7. Depry C, Allen MD, Zhang J. Visualization of PKA activity in plasma membrane microdomains. *Mol BioSyst*. 2011;7(1):52-58. doi:10.1039/C0MB00079E.
8. Grynkiewicz G, Poenie M, Tsien RY. A new generation of  $\text{Ca}^{2+}$  indicators with greatly improved fluorescence properties. *J Biol Chem*. 1985;260(6):3440-3450.
9. Buttgereit J, Shanks J, Li D, Hao G, Athwal A, Langenickel TH, Wright H, da Costa Goncalves AC, Monti J, Plehm R, Popova E, Qadri F, Lapidus I, Ryan B, Özcelik C, Paterson DJ, Bader M, Herring N. C-type natriuretic peptide and natriuretic peptide receptor B signalling inhibits cardiac sympathetic neurotransmission and autonomic function. *Cardiovasc Res*. 2016;112:637-644. doi:10.1093/cvr/cvw184.
10. Ghasemi A, Zahediasl S. Normality tests for statistical analysis: A guide for non-statisticians. *Int J Endocrinol Metab*. 2012;10(2):486-489. doi:10.5812/ijem.3505.

## Online Supplement: Neurotransmitter Switch in Prehypertension

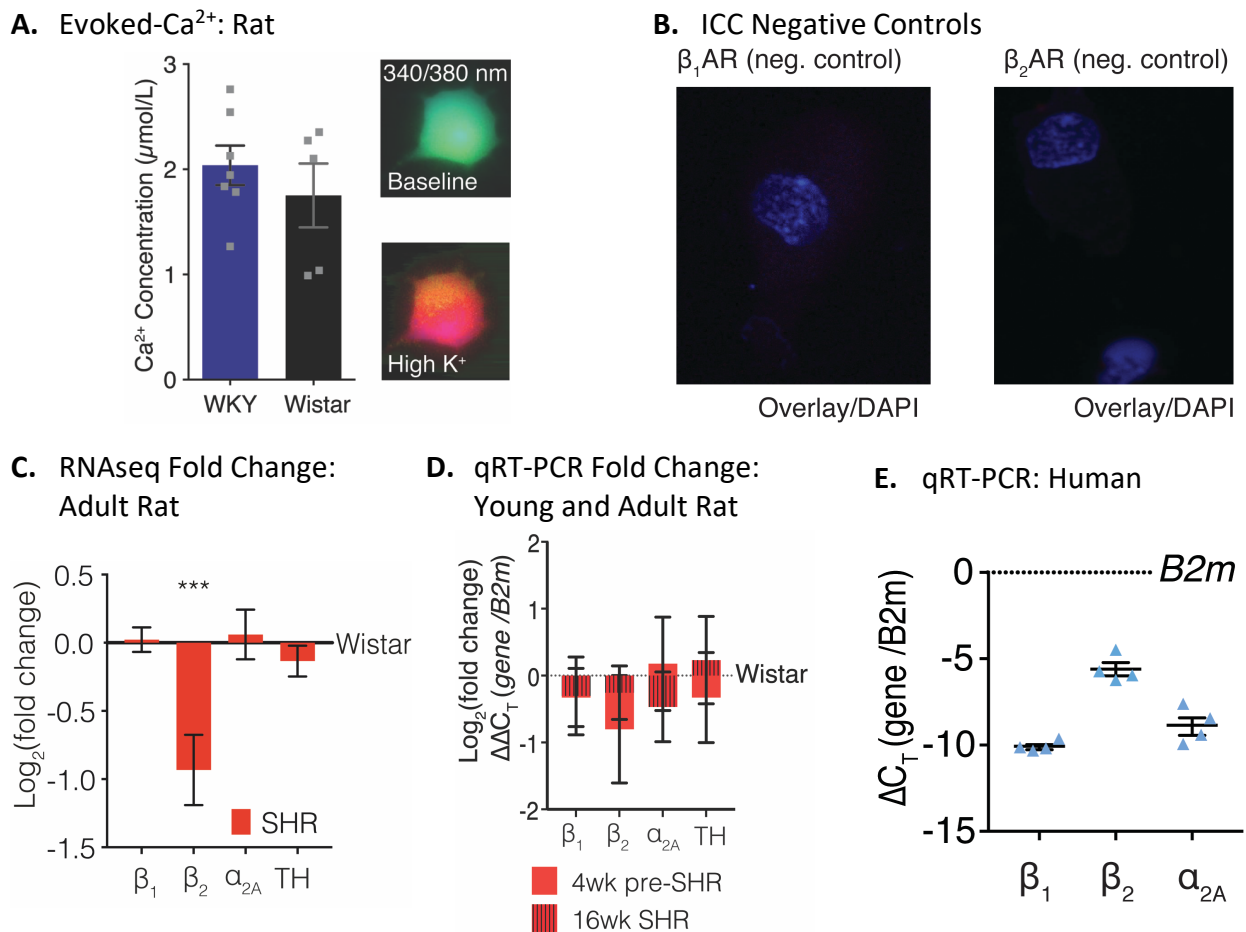
### Supplementary Results

Table S1

Characteristics of Human Donors		
Donor	Gender	Complications
#19	Male	Non-ischemic cardiomyopathy, ventricular fibrillation, LVEF 30-35%
#23	Male	None noted
#24	Male	None noted

## Online Supplement: Neurotransmitter Switch in Prehypertension

Figure S1



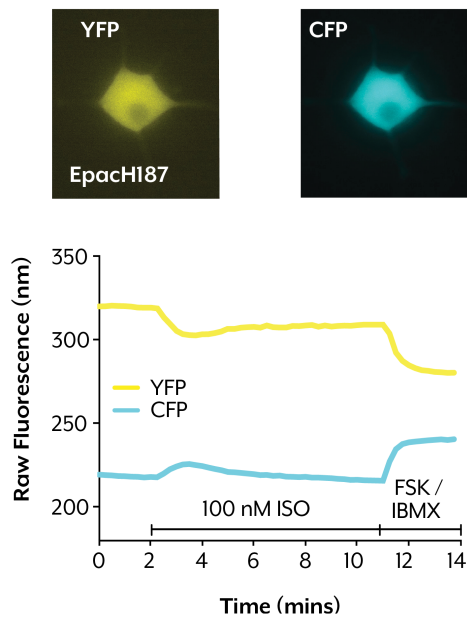
S1. There was no difference in sympathetic  $\text{Ca}^{2+}$  responses to 50 mmol/L between PGSNs obtained from 16-week Wistar or WKY rats. Given the absence of a  $\text{Ca}^{2+}$  phenotype, Wistar rats were used as the control in this study (A). For immunocytochemistry (ICC) experiments, the absence of staining with the primary antibody omitted was used as a control for nonspecific binding of the secondary antibody (B). The transcriptome of the sympathetic stellate ganglia was sequenced in 16-week old male Wistar rats ( $n=4$ ) and age-matched SHR ( $n=4$ ). Using RNAseq (C) and qRT-PCR (D) we identified the presence of  $\beta_1\text{AR}$  (*Ardb1*) and  $\beta_2\text{AR}$  (*Ardb2*) mRNA transcripts in addition to tyrosine hydroxylase (*Th*) and  $\alpha_{2A}\text{AR}$  (*Adra2a*) mRNA transcripts. In the RNAseq dataset (C) *Ardb2* expression was significantly lower in SHR ganglia compared with Wistar ( $p.\text{adj} = 0.00945$ ; Salmon-DESeq2 method<sup>4</sup>). Data points represent  $\log_2$  (fold change)  $\pm$  SEM. qRT-PCR validated the presence of transcripts in RNA extracted from 4-week ( $n=3/\text{group}$ ) and 16-week rats ( $n=4/\text{group}$ ). Fold changes were calculated by the  $\Delta\Delta\text{C}_T$  method<sup>5</sup>, where the difference in counts between the gene of interest and the housekeeping gene (*B2m*) was calculated ( $\Delta$ ). The difference between the two strains ( $\Delta\Delta$ ) was quantified and depicted as  $\log_2$  (fold change)  $\pm$  SEM. There was no significant difference in the levels of mRNA for *Adrb1*, *Adrb2*, *Adra2a* or *Th* between strains or between age groups (D). In stellate ganglia obtained from human donors (E), qRT-PCR confirmed mRNA transcripts encoding  $\beta_1\text{AR}$  (*Adrb1*) and  $\beta_2\text{AR}$  (*Adrb2*). Human stellate ganglia were also  $\alpha_{2A}\text{AR}$  positive (*Adra2a*). qRT-PCR data were analyzed by the  $\Delta\text{C}_T$  method<sup>5</sup> where data represents the difference ( $\Delta$ ) in counts relative to the housekeeping gene *B2m* (E). Individual data points represent an average (of 3 technical replicates) from one human stellate (3 patients, 4 stellates, un-pooled samples).

## Online Supplement: Neurotransmitter Switch in Prehypertension

Figure S2

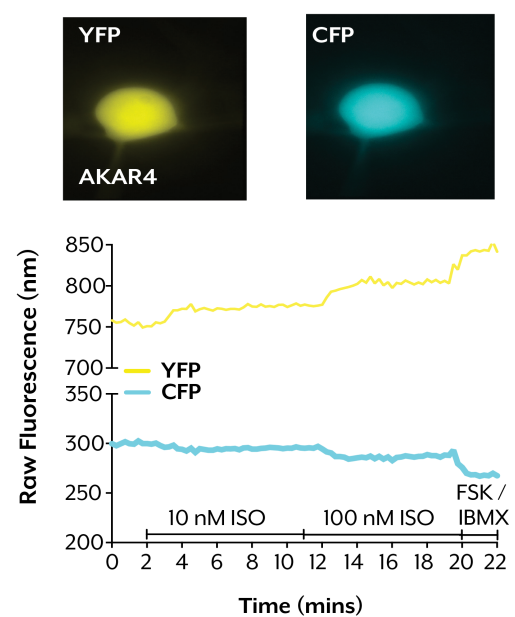
### A. EpacH187 FRET Sensor

Raw Fluorescence Example Trace: Rat

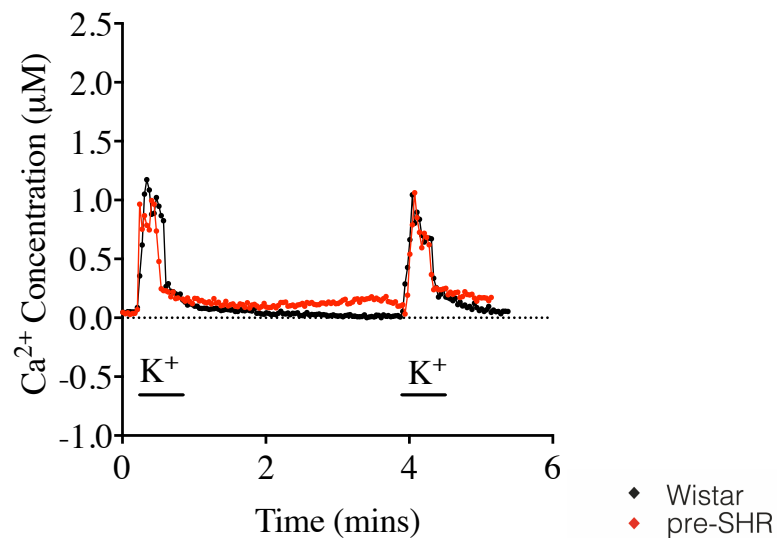


### B. AKAR4 FRET Sensor

Raw Fluorescence Example Trace: Rat



### C. $\text{Ca}^{2+}$ Imaging Time Controlled Experiment Example Trace: Rat

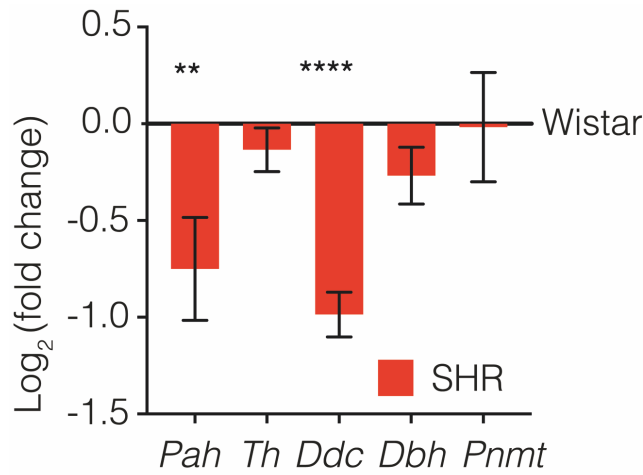


S2. Example YFP and CFP fluorescence traces over-time, as emitted from the cytosolic FRET sensors: EpacH187 (A) and AKAR4 (B) in response to ISO (10-100 nmol/L). Live  $\text{Ca}^{2+}$  imaging was conducted on PGSNs obtained from 4-week control and pre-SHR PGSNs with Indo-1AM. A time-controlled raw fluorescence  $\text{Ca}^{2+}$  trace is displayed (C). In time-controlled experiments, Wistar and pre-SHR PGSNs ( $n = 5, 6$  respectively) were exposed to two KCl stimulations (50 mmol/L; S1,  $t = 0.25$  mins; S2,  $t = 4$  mins). There was no significant difference in  $\text{Ca}^{2+}$  responses to high  $\text{K}^+$  between strains, or between stimulation 1 and 2 independent of strain.

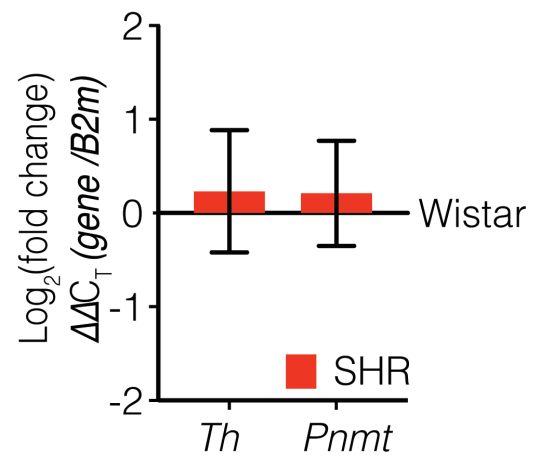


Figure S3

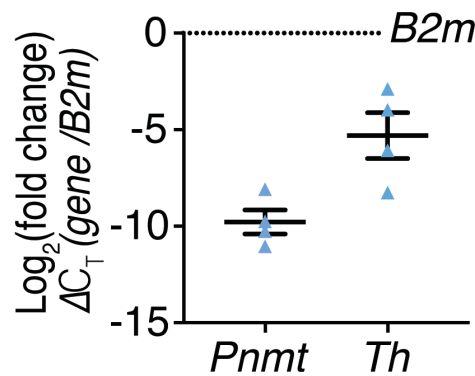
**A. RNAseq Fold Change: Adult Rat**



**B. qRT-PCR Fold Change: Adult Rat**



**C. qRT-PCR: Human**



S3. Using RNAseq we identified the mRNA transcripts encoding enzymes required for norepinephrine (NE) synthesis: phenylalanine hydroxylase (*Pah*), Tyrosine Hydroxylase (*Th*), L-DOPA decarboxylase (*Ddc*), Dopamine  $\beta$ -hydroxylase (*Dbh*) and Phenylethanolamine-N-methyltransferase (*Pnmt*); the enzyme required for the conversion of NE to epinephrine (*Epi*). *Pah* and *Ddc* transcripts are significantly lower in SHR PGSNs ( $p_{adj}=0.0719$  (*Pah*);  $6.64 \times 10^{-15}$  (*Ddc*); Salmon-DESeq2 method<sup>4</sup>). mRNA transcripts are represented as Log<sub>2</sub>(Fold change)  $\pm$  SEM (A). The presence of *Pnmt* and *Th* was confirmed by qRT-PCR in PGSNs from 4-week and 16-week Wistar and SHR. Data were normalized to *B2m* using the  $\Delta\Delta C_T$  method<sup>5</sup> and expressed as Log<sub>2</sub> (Fold change)  $\pm$  SEM (B). In human stellates, qRT-PCR confirmed the presence of *Th* and *Pnmt* (C). Data were normalized to a control housekeeping gene *B2m* using the  $\Delta C_T$  method<sup>5</sup> where the data represents the difference ( $\Delta$ ) in counts relative to the house keeping gene  $\pm$  SEM (C). Individual data points represent an average (of 3 technical replicates) from one human stellate (3 patients, 4 stellates, un-pooled samples).